DEMOCRATIC AND POPULAR REPUBLIC OF ALGERIA
MINISTRY OF HIGH EDUCATION AND SCIENTIFIC RESEARCH
UNIVERSITY OF MOHAMED BOUDIAF - M'SILA

FACULTY OF SCIENCES
DEPARTMENT OF PHYSICS

N° :PH/MAT/12/2021

DOMAINE: SCIENCE OF MATTER
FIELD : PHYSICS
OPTION : MATERIAL PHYSICS

Memory Submitted for Obtaining
Diploma of Academic Master

Prepared by: MOUSSA Hizia

TITLE :

Structural, electronic and optical properties of Ag-based oxides XAgO (X= Li and Na): An ab initio study

Defended on: 23/06/2021 before the jury composed of:

BOUSSENDEL Abdelmadjid	**University of Msila**	**President of the jury**
ALLALI Djamel	**University of Msila**	**Supervisor**
AMARI Rabie	**University of Msila**	**Examiner**

Academic Year: 2020/2021

Acknowledgement

I would first like to thank God for giving us the patience, courage and strength to do this work.

My special thanks go to Professor Djamel Allali my memory coach for his kindness, for his advice and for guiding us step by step in our work.

I would like to thank the Professor Boussendel abdelmadjid for agreeing to review this work .

I also thank the Professor Amari Rabie for the honor of chairing the jury.

Finally, I would like to thank anyone who has helped me in any way in this brief.

Thank you all

Dedication

My first dedication is addressed to my dearest mother and to my dearest father and my beautiful mother and father

To my dear husband Choayb who always encourages me.

To my beloved son Ammar youcef

To my dear sisters and brother

To my whole family

To all my loved ones.

To those who gave me everything in return.

Moussa Hizia

Contents

Introduction

One of the most advantageous and easiest ways of predicting new materials is ab initio calculations (i.e. the first principles). The term ab initio is Latin for "from the beginning". This name is given to calculations derived directly from theoretical principles without the inclusion of experimental data. The materials are composed of atoms as building units. The atoms themselves are made up of electrons. The idea behind the first principles is to apply the fundamental laws of physics to identify the behavior of a material by performing electronic structure calculations.

The so-called ab initio methods for electronic structure calculations are widely used in modern science. They allow us to simulate and sometimes even predict the properties of actual materials without using adjustable parameters. These methods require practically no information about the system; it is necessary to use only atomic numbers and coordinates as input to start the calculation. Then, all the properties of materials such as cohesive energy, equilibrium crystalline structure, phase transitions, transport properties, magnetism, ferroelectricity, optical properties and others can be extracted from the calculation and sometimes directly compared to experimental data

The ab initio study was only relatively recently possible with the development of reliable computer algorithms and the availability of high performance parallel computing facilities. Ab initio calculations can be done now on systems that only a few years ago could only be processed with semi-empirical or empirical methods.

Noncentrosymmetric(NCS) oxide compounds are of particular interest because of their symmetry-dependent properties such as pyroelectricity, piezoelectricity, ferroelectricity and second-order nonlinear optical (NLO) behaviour and are the basis for numerous applications. Classification of NCS compounds and the categories coming under these classes are given in literature [1]. At ambient conditions AMO(A=Li, Na, K and Rb; M=Ag and Cu) compounds are found to crystallize intetragonal KAgO-type structure [2–4], which comeunder NCS non-polar crystal category. They have the symmetry-dependent properties such as piezoelectric and optical activity. During last two decades, aparticular attention has been paid to piezoelectric materials due to their wide technological applications where piezoelectric materials are used as the basis materials for actuators as well as sensors. Also oxocuprates have attracted considerable attention after the discovery of high-temperature oxide superconductors and many oxocuprates have been discovered as by-products of superconductivity research [5].

The memoire is organized as follows:

In the first chapter, we present the main characteristics of the ab-initio calculations. Single-particle self-consistent field methods (Hartree and Hartree-Fock) are discussed as approximations of the multi-body Schrödinger equation. The Hohenberg-Kohn-Sham formulation of the functional theory of density is introduced. The second chapter explains the role of pseudopotential methods of the plane wave in solving Kohn-Sham equations for periodic systems. In addition, a refresher of basic solid-state physics (crystal lattices, reciprocal space, Bloch theorem . . .) is given. In the third chapter , the results of the calculations determining the properties of the LiAgO and NaAgO are presented.

Finally, the work is summarized in the Conclusion chapter ,the results of the calculations determining the Structural, electronic and optical properties of the LiAgO and NaAgO are presented.

References

[1] P. Shiv Halasyamani, Kenneth R. Poeppelmeier, Chem. Mater. 10 (1998) 2753–2769.

[2] Von H. Klassen, R. Hoppe, Z. Anorg. Allg. Chem. 485 (1982) 101–114.

[3] W. Losert, R. Hoppe, Z. Anorg. Allg. Chem. 524 (1985) 7–16.

[4] D. Fischer, W. Carl, H. Glaum, R. Hoppe, Z. Anorg. Allg. Chem. 585 (1990) 75–81.

[5] H.K. Muller-Buschbaum, Angew. Chem. 30 (1991) 723–744.

Chapter I

Fundamentals of the Density Functional Theory

I.1 Introduction

In this chapter, we briefly present the basic concepts such as the Born-Oppenheimer approximation that can be used to the separation of electronic and nuclear motions, the Variational Principle and Hartree-Fock (HF) that are used in all ab initio methods and which allow a considerable simplification of the solution of the Schrödinger equation. This naturally leads to the introduction of the functional theory of density, one of the most popular methods for the solution of the many-body problem.

I.2 Solving the Schrödinger equation

All materials are composed of atomic nuclei and electrons which determine the physical properties of materials and molecules: whether, for example, they are hard or soft, reactive or inert, conducting or insulating, superconducting or magnetic, good at converting solar radiation to more useful forms of energy or not. In non-relativistic quantum mechanics, the ground state of a system of atomic nuclei surrounded by electrons can be described by solving the time-independent Schrödinger equation, which has the form [1, 2]:

$$H\psi(\{R_I\},\{r_i\}) = E\psi(\{R_I\},\{r_i\}) \quad \text{(I. 1)}$$

Where E is the total energy of the system, Ψ is the many-body wave function , $\{R_I\}$ is the set of nuclear coordinates and $\{r_i\}$ those describing the 'electrons and H is the Hamiltonian of the system composed of n electrons and N nuclei with charges Z_I. This Hamiltonian is given by

$$\widehat{H} = \hat{T}_e + \widehat{T_n} + \widehat{V_{ee}} + \widehat{V_{ne}} + \widehat{V_{nn}} \quad \text{(I. 2)}$$

In equations (I.2):

The first term $\hat{T}_e = -\frac{\hbar^2}{2m_e}\sum_{i=1}^{n}\nabla_{r_i}^2$ represent the kinetic energy operator for the electrons

The second term $\widehat{T_n} = -\frac{\hbar^2}{2M_I}\sum_{I=1}^{N}\nabla_{R_I}^2$ represent the kinetic energy operator for the nuclei,

The third term $\widehat{V_{ne}} = -\sum_{I}^{N}\sum_{i}^{n}\frac{1}{4\pi\varepsilon_0}\frac{Z_I e^2}{|R_I - r_i|}$ is the coulombic interaction between electrons and nuclei,

The fourth term $\widehat{V_{ee}} = \frac{1}{2}\sum_{i\neq j=1}^{n}\frac{1}{4\pi\varepsilon_0}\frac{e^2}{|r_i - r_j|}$ is the electron-electron Coulomb repulsion energy,

And the last term $\widehat{V_{nn}} = \frac{1}{2}\sum_{I\neq J=1}^{N}\frac{1}{4\pi\varepsilon_0}\frac{Z_I Z_J e^2}{|R_I - R_J|}$ is the nucleus-nucleus Coulomb repulsion energy.

Where i and I are the indices of electrons and nuclei, respectively, r_i and R_I are the coordinates of electrons and nuclei, respectively, m and e are the mass of the electron and the charge of the electron , respectively, M_I and Z_I are the mass and the charge of the I-th nucleus,

respectively, and $\hbar$ is the Planck constant, $\varepsilon_0$represents the permittivity of the vacuum, $|r_i - r_j|$ represents the distance between the electrons i and j, $|R_I - r_i|$ represents the distance between the i-th electron and the I-th nucleus / ion and $|R_I - R_J|$ is the distance between the I-th and the J-th nucleus / ions.

Throughout this thesis, we shall use the so-called Hartree atomic units in which mass is reckoned in units of the electron mass (m_e = 9.1093826 × 10^{-31} kg) and distance in terms of the Bohr radius (a_0=5.299175×10^{-2}nm), such that($\hbar = e = m_e = 4\pi\varepsilon_0 = 1$), the Hamiltonian is written in the most convenient form:

$$\hat{H} = -\frac{1}{2}\sum_{i=1}^{n}\nabla_{r_i}^2 - \frac{\hbar^2}{2M_I}\sum_{I=1}^{N}\nabla_{R_I}^2 - \sum_I^N\sum_i^n\frac{Z_I e^2}{|R_I - r_i|} + \frac{1}{2}\sum_{i\neq j=1}^{n}\frac{e^2}{|r_i - r_j|} + \frac{1}{2}\sum_{I\neq J=1}^{N}\frac{Z_I Z_J e^2}{|R_I - R_J|} \quad (I.3)$$

In principle, Solving Equation (I.1) is the perfect way to determine any physical property of a system of many particles. However, in practice, it is virtually impossible to solve such a complex equation, either analytically or numerically. This is due to the complexity of the above Schrödinger equation and the extremely large number of variables involved in the problem. Only for a few cases, such as hydrogen-like ions or the H_2^+ molecule, a complete analytic solution is available. The challenge posed by the many-body problem in quantum physics originates from the difficulty of describing the non-trivial correlations encoded in the exponential complexity of the many-body wave function. The many-body wave function must not only reflect the Coulomb interactions between the particles, but must also obey antisymmetry with respect to the exchange of two particles. Hence, the quantum many-body problem is centred upon finding intelligent approximations for the Hamiltonian (I.3) and the many-body wavefunction ψ ,that render the Schrodinger equation tractable to numerical solution, while retaining as much of the key physics as is possible. The first approximation is to separate degrees of freedom from nuclear and electronic movements by using the Born-Oppenheimer approximation [3].

I.2.1 The Born-Oppenheimer approximation

The concept behind the Born-Oppenheimer approximation, also called adiabatic approximation [3], comes from the huge difference of mass between ions and electrons, the masses of the nuclei, being approximately two thousand times greater than those of the electrons. Typically, the ions can be considered as moving slowly in space and the electrons responding instantaneously to any ionic motion so that electrons can immediately find their ground state while the nuclei move. Hence, it seems plausible to neglect the kinetic energy of

the nuclei in zeroth order, and we take into account their kinetic energy as a classic contribution. This considerably reduces the complexity of the calculations because the presence of the kinetic term associated with the nuclear motion makes the study of the hypothetical many-body *system* into a very complex problem. It should be mentioned that the electronic properties always depend on the position of the nuclei, but not on their dynamics, such that the electronic properties depend parametrically on the position of the nuclei. The Coulomb potential describing the interaction between electrons and nuclei is therefore considered as an external potential.

Under the Born-Oppenheimer approximation, the total wave function $\Psi(\{r_i\},\{R_I\})$ can be approximated as the product of a nuclear wavefunction and an electronic wavefunction:

$$\Psi(\{r_i\},\{R_I\}) = \Psi_{ion}(\{R_I\})\Psi_{el}(\{r_i\},\{R_I\}) \quad (I.4)$$

Where $\Psi_{ion}(\{R_I\}$ is the nuclear wavefunction, and $\Psi_{el}(\{r_i\},\{R_I\})$is the many-electron wave function that depend on the simultaneous coordinates of all the electrons .After some manipulation, we can write the Schrödinger equation only for the electrons at a given nuclear coordinates as:

$$H_e\Psi_{el}(\{r_i\},\{R_I\}) = E_e\Psi_{el}(\{r_i\},\{R_I\}) \quad (I.5)$$

With

$$H_e = -\frac{1}{2}\sum_{i=1}^{n}\nabla_{r_i}^2 - \sum_{I=1}^{N}\sum_{i=1}^{n}\frac{Z_I}{|R_I-r_i|} + \frac{1}{2}\sum_{i\neq j=1}^{n}\frac{1}{|r_i-r_j|} \quad (I.6)$$

For all given nuclear coordinates (R_I), the obtained electronic wave function $\Psi_{el}(\{r_i\},\{R_I\})$ depends parametrically on (R_I), and it will change when the nuclei are moved.

The total energy of the system (electrons- nuclei) at any (static) set of (R_I) is a sum of electronic energies E_e and nuclear energies due to nucleus-nucleus interaction:

$$E_{tot}(\{R_I\}) = \langle\Psi_{el}|H_e|\Psi_{el}\rangle + V_{nn} \quad (I.7)$$

The last V_{nn}term enter only as a constant in each considered geometry.

If we know E_{tot} for many sets of nuclear coordinates, the nuclei movement can be described by the nuclear Hamiltonian H_n :

$$H_n = T_n + E_{tot}(\{R_I\}) = T_n + \langle\Psi_{el}|H_e|\Psi_{el}\rangle + V_{nn} \quad (I.8)$$

The Schrödinger equation for nuclei is given

$$\left(-\frac{\hbar^2}{2M_I}\sum_{I=1}^{N}\nabla_{R_I}^2 + E_{tot}(\{R_I\})\right)\Psi_{ion}(\{R_I\}) = E_{Nu}\Psi_{ion}(\{R_I\}) \quad (I.9)$$

Note that Hamiltonian eigenvalues for nuclear motion are total energies for the system because they contain the electronic energy in their potential parts, therefore:

$$E_{tot} = E_{nuc} \quad (I.10)$$

Under the Born-Oppenheimer approximation, the dimension of the problem is reduced and the calculation is associated only with electronic degrees of freedom. However, the spatial dimension is still too important for real compounds. For a system of N electrons, the wave function $\Psi_{el}\ (\{r_i\}) \equiv \Psi_{el}\ (r_1, \ldots, r_N)$ depends on 3N spatial variables. This causes a rapid increase in the complexity of the problem with the size of the system. Already for the small systems, which consist only of dozens of electrons, the calculation becomes unfeasible. Moreover, the equation above contains a two-particle interaction in the form of the electron-electron potential. Therefore, under the Born-Oppenheimer approach, the solution of Equation (I.5) for electrons is still a problem of many-body. We need to do more, before simulations are done. For weak interaction systems, a perturbative approach might be the best solution, but if we want good results in general, we need another method.

I.2.2 The Hartree approximation

The first approach to the problem of many electrons can be considered as that proposed by Hartree (1928) [4]. The basic assumption of this approximation is that the many-electron wave function can be written as a simple product of *N* monoelectronic wave functions, even when the electron-electron interactions are not neglected.

$$\Psi(r_1, r_2 \ldots, r_N) = \psi(r_1)\psi(r_2) \ldots \psi(r_N) \qquad (I.11)$$

The $\psi(r_i)$ are the N independent electronic wave functions. This approximation defines the potential by separating it into an electron potential (V_{elec}) and an ion potential V_{ion}. During the interaction, a given electron is no longer subject to a potential depending on the instantaneous positions of all other electrons, but rather to a potential corresponding to the average electron distribution, so that the remaining electrons are treated as a regular distribution of the negative charge with their charge density. We can say that the electron moves in an average electrostatic potential $V_H(r)$ from the set of neighboring electrons, so that eventually we would be able to process a non-interacting particle system instead of processing particles in interaction. With this approximation, the energy of the system can be written as [5]:

$$E^H = \langle \Psi | \hat{H} | \Psi \rangle$$

$$= \sum_i^n \left\langle \psi(r_i) \left| \frac{1}{2}\nabla_{r_i}^2 + V_{ion}(r) \right| \psi(r_i) \right\rangle + \frac{1}{2}\sum_{i,j(i\neq j)}^n \left\langle \psi(r_i)\psi(r_j) \left| \frac{1}{|r_i - r_j|} \right| \psi(r_i)\psi(r_j) \right\rangle \qquad (I.12)$$

Applying the Variational principle, we obtain the Hartree equation to a single particle:

$$\left[\frac{1}{2}\nabla_{r_i}^2 + V_{ion}(r) + \sum_{i,j(i\neq j)}^n \left\langle \psi(r_j) \left| \frac{1}{|r_i - r_j|} \right| \psi(r_j) \right\rangle\right] \psi(r_i) = \varepsilon_i \psi(r_i) \qquad (I.13)$$

Where $V_{ion}(r)$ represents the Coulomb potential resulting from the interaction of the electron at the position r_i with all nuclei and $\sum_{i,j(i\neq j)}^{n}\left\langle\psi(r_j)\right|\frac{1}{|r_i-r_j|}\left|\psi(r_j)\right\rangle$ represents the Coulomb potential resulting from the interaction of this electron with all other electrons, this term is commonly referred to as Hartree potential.

By introducing the concept of the atomic density of electrons $\rho(r_j)$,Hartree defined the potential that an electron experience by using the following relation:

$$V_H(r_i)=\langle\sum_{j\neq i}^{n}\frac{1}{|r_i-r_j|}\rangle=\int\frac{\rho(r_j)}{|r_i-r_j|}d^3r_j \qquad (I.14)$$

Where the density of probability ρ at the position r_j is given by the absolute square of the wave function $\psi_j(r)$, and the integration is carried out over the coordinates of all the electrons except over the coordinate r_i of the electron i:

$$\rho(r_j)=\sum_{j\neq i}^{occ}\left|\psi_j(r)\right|^2 \qquad (I.15)$$

The Hartree potential can be obtained also from the Poisson equation:

$$\nabla^2V_H=-4\pi e^2n(r) \qquad (I.16)$$

The Hartree equation is written as

$$H_i\psi(r_i)=\varepsilon_i\psi(r_i) \qquad (I.17)$$

With

$$H_i=\frac{1}{2}\nabla_{r_i}^2+V_{eff}(r_i) \qquad (I.18)$$

Where

$$V_{eff}(r_i)=V_{ion}(r_i)+V_H(r_i) \qquad (I.19)$$

Solving the equation (I.17) yields all ε_i and $\psi(r_i)$.

The total Hamiltonian is simply a sum of one-electron operators, H_i.

$$H_e=\sum_i^N H_i \qquad (I.20)$$

This implies that the total energy of the electronic system E_e is the sum of the energies of the separated electrons:

$$E_e=\sum_i^N\varepsilon_i \qquad (I.21)$$

Equation (I.17) has a very familiar form and it is similar to the Schrödinger equation for a single electron moving in an effective potential $V_{eff}(r_i)$. However, there is a big difference: in the Hartree equation, the potential depends on the solution itself, in order to solve the equation (I.17) for each wave function $\psi(r_i)$, all the other functions $\psi(r_j)$ must be known, that requires a self-consistent method. First, a set of approximate wave functions $\psi(r_j)$ is chosen as a test set from which the N one-electron functions and the V_H potential are calculated. By inserting the

potentials V_H in equation (I.17), one can obtain the solutions of the Hartree equation. Then, using these solutions, we recalculate the potentials V_H and the equation is solved again and the potential is calculated. This procedure is repeated until the input and the output potentials are very close, within a certain tolerance.

The disadvantage of Hartree approach is that he does not take into account the Pauli Exclusion Principle [6], which requires that two electrons cannot be in the same quantum state.

The introduction of this principle (the inclusion of exchange) transforms the Hartree approach into the Hartree-Fock approximation [7].

I.2.3 The Hartree-Fock approximation

The Hartree-Fock approximation [7] follows directly from what was done for the Hartree approximation, only taking into account the need for the antisymmetric character of the wave functions with respect to electron exchange, as required by the principle of exclusion of Pauli [6].This could be achieved by adding and subtracting all possible permutations of the Hartree product. The wave function becomes the function of the 4N variables (the three coordinates and the spin of the electron).

In the framework of the Hartree Fock approximation [7], the many-body wave function is assumed to be a single Slater determinant of single-particle orbitals [8]:

$$\Psi_{HT} = \frac{1}{\sqrt{N!}}\begin{vmatrix} \psi_1(x_1) & \psi_2(x_1) & \dots & \psi_N(x_1) \\ \psi_1(x_2) & \psi_2(x_2) & \dots & \psi_N(x_2) \\ \vdots & \vdots & \vdots & \vdots \\ \psi_1(x_N) & \psi_2(x_N) & \dots & \psi_N(x_N) \end{vmatrix} \qquad (I.22)$$

Where x_i in the wave functions represents all the coordinates (space and spin) of particle i,

The total energy with the Hartree-Fock wave function is obtained by:

$$E^H = \langle \Psi | \hat{H} | \Psi \rangle = \sum_{i=1}^{N} H_i + \frac{1}{2}\sum_{i,j=1}^{N}(J_{ij} - K_{ij}) \qquad (I.23)$$

Where

$$H_{ii} = \int \psi_i^*(x_i)\left[\frac{1}{2}\nabla_{r_i}^2 + V_{ion}(r)\right]\psi_i(x_i)\,dx$$

$$J_{ij} = \iint \psi_i(x_1)\psi_i^*(x_1)\frac{1}{r_{12}}\psi_j^*(x_2)\psi_j(x_2)\,dx_1dx_2 \qquad (I.24)$$

$$K_{ij} = \iint \psi_i^*(x_1)\psi_j(x_1)\frac{1}{r_{12}}\psi_i(x_2)\psi_j^*(x_2)\,dx_1dx_2$$

Where the J_{ij} are called Coulomb term and K_{ij} is the exchange term. We have significant equality: $J_{ij} = K_{ij}$ .The exchange term is similar to the direct Coulomb term, but for the exchanged indices

Hartree-Fock equations with a single particle are obtained by a Variational calculus [9]:

$$\hat{F}\psi_i(x) = \varepsilon_i\psi_i(x) \qquad (I.25)$$

Where

$$\hat{F} = \hat{h}_i + \sum_{j=1}^{N}(\hat{J}_j - \hat{K}_j) \qquad (I.26)$$

Where $\hat{h}_i$contains the kinetic energy of the electron i and its interaction with all the nuclei. The second term in equation (I.26) is the Coulomb operator $\hat{J}_j$ and it represents the potential that an electron in position x_1 experiences due to the average charge distribution of another electron in the orbital of spin $\psi_j$and it is defined by its effect when it operates on a spin orbit by:

$$J_j\psi_i(x_1) = \left(\int \frac{|\psi_j(x_2)|^2}{r_{12}}\, dx_2\right)\psi_i(x_1) \qquad (I.27)$$

The last term $K_j$is the exchange operator. It stems from Pauli's exclusion principle and acts to separate electrons in the same spin state. This term has no classical analogue and is a purely quantum mechanical effect, caused by the anti-symmetric ansatz of the wave function when interchanging any two electrons, it is best represented by showing how it acts on a single particle wave function

$$K_j\psi_i(x_1) = \left(\int \frac{\psi_j^*(x_2)\psi_i(x_2)}{r_{12}}\, dx_2\right)\psi_j(x_1) \qquad (I.28)$$

By multiplying the equation (I.23) by ψ_i^* and integrating, we obtain for the Hartree-Fock spin-orbital energies the following expression:

$$\varepsilon_i = \langle\psi_i|\hat{F}|\psi_i\rangle = H_{ii} + \sum_{J=1}^{N}(J_{ij} - K_{ij}) \qquad (I.29)$$

The approximate electronic energy of the electronic ground state is then calculated as:

$$E_{HF} = \sum_{i=1}^{N}\varepsilon_i - \frac{1}{2}\sum_{i=1}^{N}\sum_{j=1}^{N}(J_{ij} - K_{ij}) \qquad (I.30)$$

And for total energy, including nuclear-nuclear repulsion [9] we obtained:

$$E_{tot} = \sum_{i=1}^{N}\varepsilon_i - \frac{1}{2}\sum_{i=1}^{N}\sum_{j=1}^{N}(J_{ij} - K_{ij}) + V_{nn} \qquad (I.31)$$

The Hartree-Fock approach is widely used by quantum chemists today. However, it has limitations, the Hartree-Fock equation is difficult to apply in extended systems because of its exchange term, which is non-local. The computational complexity of the Hartree-Fock method grows rapidly with the number of atomic electrons, so the corresponding calculated time for heavy atoms is found to be too long even when using modern computers. For this reason, there

has been relatively few applications to solids [10]. In addition, the Hartree-Fock approximation sometimes gives unsatisfactory results because the approximation of an electron no longer takes into account the quantum effects on the electron distributions because the effect of other electrons in the system on an electron of interest is processed according to their average location. It does not consider instant Coulomb interactions between electrons. The Hartree-Fock equations neglect more detailed correlations due to many-body interactions. Much of the modern work in the field of calculating the electronic structure is designed to take electronic correlation into account.

I.3 The theory of the density functional

The alternative of HF methods is the density functional theory (DFT), which is becoming increasingly popular in condensed matter physics, quantum chemistry and materials science. The main idea of the density functional methods is that the problem is solved directly for the charge density, ρ(r) rather than for the wave function Ψ of several particles [11]. This leads to a remarkable reduction in the difficulty because it is enough to treat a function of three variables x, y and z, rather than a problem of 3N variable.

Density functional theory (DFT) not only had a major impact on structural-electronic calculations, but it also makes it possible to treat properties of rather complex materials. This involves the determination of magnetic and electrical susceptibilities, spin-polarized fundamental states, superconductivity, etc. [11]. On the other hand, density functional theory (DFT) is a good compromise between the qualitative description of the electronic structure and the computational efficiency required to produce the result.

The density functional theory has its roots in Thomas and Fermi's publications in the 1920s. Thomas and Fermi [12, 13] have attempted to formulate such an approach much earlier; however, their work, suffered from inaccuracies in the processing of kinetic energy and exchange-correlation effects. Nevertheless, the method served as a starting point for the development of more advanced publications in the early 1960s [14, 15].

In their 1964 article, Hohenberg and Kohn formulated the basics of density functional theory for any system of N electrons moving in an external potential V_{ext} (r) and whose fundamental state is nondegenerate. The Hamiltonian operator for such a system can be written as:

$$\hat{H} = \hat{F} + \hat{V}_{ext} \qquad (I.32)$$

Where

$$\hat{F} = -\frac{1}{2}\sum_{i=1}^{N} \nabla_i^2 + \sum_{i\neq j}^{N} \frac{1}{|r_i - r_j|} \qquad (I.33)$$

and

$$\hat{V}_{ext} = \sum_{i=1}^{N} V_{ext}(r_i) = -\sum_{i=1}^{N}\sum_{i\neq j}^{M} \frac{Z_j}{|r_i - R_j|} \qquad (I.34)$$

Hohenberg and Kohn outlined DFT in terms of two theorems, proving the existence of a one-to-one mapping between the potential V (r) and the density n (r).

I.3.1 Hohenberg-Kohn's theorem

I.3.1.1 Hohenberg-Kohn's first theorem

The first theorem of Hohenberg and Kohn states the following: [14]

The ground state density ρ (r) of a system of interacting electrons in an external potential V_{ext} (r) uniquely defines this potential.

In the term "unique" we must understand "unique to an additive constant". Indeed, the charge density is not modified if a constant is added to the external potential [16].

Hohenberg and Kohn have been able to prove that there is a relation of *uniqueness* between ρ (r) and the external potential: two external potentials could not give the same ρ (r). This tells us that we can derive the potential External V_{ext} (r) applied to an interacting N *electron system* from the electronic density of this *system*. In addition, all the properties of a system can be determined also via the electronic density of the system. This formulation can be applied to any particle system interacting in an external potential, including fixed-core problems and electrons. Originally, this theorem has been demonstrated for nondegenerate states, then it has been extended to a vast class of systems including degenerate state systems [17, 18], spin-polarized systems [19, 20]. This theorem has also been extended to finite temperature by Mermin [21], thus proving that entropy, specific heat, etc. are functionals of the equilibrium density [22].

I.3.1.2 Second theorem of Hohenberg-Kohn

The second theorem of Hohenberg-Kohn is directly related to the first and indicates that*: There exists a universal functional F [ρ(r)] of the density, valid for any external potential Vext(r), such that the global minimum value of the energy functional* $E_{tot}[\rho] = F_{HK}[\rho] + \int dr \hat{V}_{ext}\,\rho(r)$ *is the exact ground state energy of the system and the density n(r) that minimizes this functional is the exact ground state density* $\rho_0(r)$*. Thus, the exact ground state energy and density are fully determined by the functional E[ρ (r)]*.

$F_{HK}[\rho]$ is a universal functional valid for any number of electrons having an external potential, in the sense that $F_{HK}[\rho]$does not depend on the external potential felt by the electrons (not including any information on the nuclei or on their positions).

$F_{HK}[\rho]$ contains the kinetic term of the interacting particles $\hat{T}_e$and the energy of the interaction between the electrons, $\hat{V}_{ee}$

$$F_{HK}[\rho] = \hat{T}_e + \hat{V}_{ee} \qquad (I.35)$$

If the form of the "true" functional was known, we could vary the electron density until the energy functional is minimized. The electronic density that minimizes the total energy functional is the true density (the ground-state density) corresponding to the energy of the ground state of the system. This means that we can think of solving the Schrödinger equation by finding the electronic density, which is a function of three spatial variables, rather than the wave function, which is a function of 3N variables.

The Hohenberg-Kohn theorem does not tell us the form of the functional of energy as a function of density: it only proves that such a functional exists.

The next major step in the development of DFT came with the derivation of a set of one-electron equations from which the electron density ρ (r) can be obtained [15].

I.3.2 Kohn and Sham's approach

Based on the fact that Hohenberg and Kohn's theorems are valid for any electronic system, whether interacting or not, Kohn and Sham (1965) [15] introduced an elegant method that became the most practical implementation of the density functional theory. Their idea is to replace formally the "real" electrons of a system by an auxiliary system of non-interacting electrons (Vee = 0) evolving as independent particles in an effective potential so that the charge density in this auxiliary system is exactly the same as in the full interacting system [22].

The important achievement of Kohn and Sham was to write the energy functional for the real system as:

$$E_{HK}[\rho] = \langle \Psi | \hat{T}_e + \hat{V}_{ee} + \hat{V}_{ext} | \Psi \rangle$$
$$= T_e^{KS} + E_{Hartree}[\rho] | \Psi \rangle + \int \rho(r) V_{ext} dr + E_{XC}[\rho] \qquad (I.36)$$

The first term T_e^{KS} is the functional of the kinetic energy for a set of N non-interacting electrons with the same ground-state density ρ (r) as the interacting one. But T_e^{KS} is not equal to the true kinetic energy of the interacting electron system. The interest of the introduction of this fictitious system is that we can now express the functional kinetic energy as a function of the orbitals ψ_i.

If each effective electron is described by a single particle wave function ψ_i, the kinetic energy of all effective electrons is given by:

$$T_e^{KS}[\rho(r)] = \frac{1}{2}\sum_{i=1}^{N}|\nabla\psi_i(r)|^2 \quad (I.37)$$

Where the sum is on all occupied orbitals of Kohn-Sham (KS).

The second term is the functional of the electrostatic energy, commonly known as the Hartree contribution; it is purely classical and contains the electrostatic energy arising from the repulsion between all electronic charges,

$$E_H(\rho) = \int \frac{\rho(r_i)\rho(r_j)}{|r_i - r_j|} dr_i\, dr_j \quad (I.38)$$

The third term is the classical electron-nuclei Coulomb interaction with the potential $V_{ext}\rho(r)$ due to the nuclei i.e.

$$E_{ext}[\rho] = \int V_{ext}\rho(r)dr \quad (I.39)$$

$$V_{ext}(r) = -\sum_{j=1}^{M}\frac{Z_j}{|r - R_j|} \quad (I.40)$$

Where Z_j is the positive charge of the nucleus in R_j.The fourth term is a universal functional, termed: the exchange–correlation functional. It groups all remaining complicated electronic contributions to make the functional in Eq. (I.36) exact, however, its exact form is not known. It contains the difference between the exact kinetic energy T[ρ(r)] and non-interacting kinetic energies T_e^{KS}as well as the non-classical part of $V_{ee}[\rho(r)]$:

$$E_{xc}[\rho] = T[\rho(r)] - T_e^{KS}[\rho(r)] + V_{ee}[\rho(r)] - V_H[\rho(r)] \quad (I.41)$$

As the name suggests, $Exc[n]$ arises from a combination of two quantum mechanical effects: electron exchange and correlation. The most important of these contributions is the exchange term. Briefly, electron exchange arises because a many-body wave function must be antisymmetric under exchange of any two electrons since electrons are fermions and obey the Pauli Exclusion Principle. In real space, Pauli's principle implies that in the neighbourhood of every electron with a given spin, all other electrons with the same spin tend to avoid that electron, just as it has been postulated the existence of a (Fermi) exchange hole excluding the electrons of parallel spins in the same region of space. Consequently, the exchange term reduces the Coulomb repulsion of the electronic system by increasing the spatial separation between electrons and cancels out this unwanted interaction in a sense. Likewise, a correlation hole must be "imagined" for opposite spin electrons because the motion of each individual electron is correlated with the motion of all others and electrons with opposite spins also avoid each other, helping also to keep electrons of unlike spin spatially separated. The additional many- body interaction terms between electrons of opposite spin are called correlation energy.

I.3.3 The Kohn-Sham equations

The minimization of the total energy (equation (I.36)) with respect to density, for a fixed number of electrons, produces a set of equations:

$$\left[-\frac{1}{2}\nabla^2 + V_{eff}\right]\psi_i(r) = \varepsilon_i\psi_i(r) \qquad (I.42)$$

Here, the one-electron orbitals $\psi_i(r)$ are called the Kohn-Sham orbitals and the above eigenvalue equations are called the Kohn-Sham equations.

Where i refers to the ith electron, $\psi_i(r)$ is the single particle wave function of this electron. and $\hat{V}_{eff}(r)$ is the effective potential given by:

$$\hat{V}_{eff}(r) = \hat{V}_H(r) + \hat{V}_{ext}(r) + \hat{V}_{XC} \qquad (I.43)$$

Where

$$\hat{V}_{XC}(r) = \frac{\delta E_{XC}[n(r)]}{\delta\rho(r)}\Big|_{\rho=\rho 0} \qquad (I.44)$$

And

$$\hat{V}_H(r) = \frac{\delta E_H[\rho(r)]}{\delta\rho(r)} = \int \frac{\rho(r_j)}{|r-r_j|}dr_j \qquad (I.45)$$

The Hartree potential $\hat{V}_H(r)$ namely contains a Coulomb repulsion between an electron and itself in the sense that it interacts with a charge density constructed from its own wave function. This is clearly visible in the case of one electron where the Hartree energy is non-zero. The self-interaction of the Hartree potential is exactly cancelled by exchange-correlation hole.

The set of Kohn-Sham equations is to be solved self-consistently, under the constraint that the number of particles is conserved.

Due to the dependence of the effective potential on the density via the Hartree potential. The total energy of the system is not simply equal to the sum of the eigenvalues of the Kohn-Sham equations, but it is calculated by adding the different energy contributions with corrections for double counting:

$$E = \sum_n^N \varepsilon_n + E_{XC}[\rho] - \int V_{XC}(r)\rho(r)dr - \frac{1}{2}\iint \frac{\rho(r)\rho(r_j)}{|r-r_j|}drdr_j \qquad (I.46)$$

Where the sum over the values of a single particle is often called band structure energy. The electron density is expressed according to the orbitals

$$\rho(r) = \sum_{i=1}^N |\psi_i(r)| \qquad (I.47)$$

Where $\psi_i(r)$ are the KS orbitals that are the lowest energy solutions of the equations (I.42).

The full wavefunction of non-interacting is far less complicated that of the true interacting system and it must still satisfy exchange anti-symmetry and this can be achieved by placing single-particle wavefunctions in a Slater determinant [8].

Slater Determinant constructed from a set of KS orbitals is the exact wave function for the fictional non-interacting system having the same density as the real system.

The Kohn-Sham equations seem formally very similar to the Hartree-Fock equations. They have identical contributions to the kinetic energy and from the external potential as well as from the Coulomb energy of the electrons; the only difference is the presence of exchange-correlation potential. The Kohn-Sham equations contains both parts (the exchange and the correlation), and they are treated via an approximate treatment, whereas in the Hartree–Fock equation only exchange interactions are included and it treated exactly [23]. The Kohn-Sham equations are much easier to be solve than the Hartree-Fock equations, in which the potential depends on the orbit [24]. In the Kohn-Sham equations, the effective potential is the same for each orbit in the sense that occupied and unoccupied orbitals all feel the same effective potential $\hat{V}_{eff}(r)$.

I.3.4 The exchange–correlation potential

Kohn and Sham (KS) reformulated the problem in a more familiar form and opened the way to practical applications of DFT, but the precise dependency of the exchange–correlation potential V_{XC} on the density $\rho(r)$ is not known. Nevertheless, this exchange–correlation potential can be approached and many approximations have been proposed and tested on different types of systems. The most common approximations in solid-state physics are the local density approximation (LDA) and the generalized gradient approximation (GGA).

I.3.4.1 Local density approximation (LDA)

The simplest physical way of approaching the exchange-correlation energy is Local Density Approximation (LDA) proposed by Kohn and Sham themselves [15]. The idea behind the LDA is very simple; it simply ignores the non-local aspects of the functional dependence of Vxc and assumes that Vxc only depends on the local density ρ. So that at each point in the system, the exchange and correlation energy per particle has the value that would be given by a homogeneous electronic gas that had the same electron density ρ at *this point*. Note that the LDA does not assume that the electron density in a molecule is homogeneous (uniform); this drastic situation would be true for a "Thomas-Fermi molecule", which cannot exist. The total

exchange correlation energy E_{xc} is then given by the sum of the contributions of each point in space,

$$E_{XC}[\rho] = \int dr\, \rho(r)\varepsilon_{xc}(\rho(r)) \quad \text{(I. 48)}$$

Where$\varepsilon_{xc}(\rho(r))$ is the exchange-correlation energy per particle.

The quantity $\varepsilon_{xc}(\rho(r))$can be divided into exchange and correlation contributions represented by the energies per particle ε_X and ε_C.

$$\varepsilon_{XC}(\rho((r)) = \varepsilon_X(\rho(r)) + \varepsilon_C(\rho(r)) \quad \text{(I. 49)}$$

Both terms are negative. The exchange portion is generally larger than the correlation portion, typically by a factor of 3 to 10 in the crystallographic systems.

The exchange contribution can be evaluated analytically [22], while the correlation part is obtained by parameterizing of precise quantum Monte Carlo simulations of the homogeneous electron gas as proposed by Ceperly and Alder [25]. Depending on the analytic forms used for $\varepsilon_C(\rho(r))$, several local density approximations were have been generated, the most widely used LDA functional is that parametrized by Perdew-Zunger (PZ81) [26].

The LDA approximation is only strictly valid for interacting electron systems within the limits of a slowly varying density and very high densities. Nevertheless, experience has shown that accurate results can be obtained well beyond this expected range of validity [27]; it is surprisingly successful and even works reasonably well in systems where the electron density is rapidly varying. Typically, the LDA has proven to be a remarkable fruitful approximation in reproducing excellent numerical results for strongly bound system, which share some properties with the HEG, especially for vibrational and structural properties.

However, LDA has many short-comings mostly due to the tendency to overbind atoms (has a tendency to make chemical bindings much too strong). This leads to cell parameters being underestimated by several percent for solids. Therefore, the bulk modulus is overestimated. The main deficiency of the LDA was the large errors in predicting the energy gaps of some semi-conductors and insulators [28].

The limitations of The LDA led to the subsequent level of approximation to the exchange-correlation energy, a natural way to improve LDA is to make the exchange-correlation functional not only dependent on the local density, but also the on gradient of the density.

I.3.4.2 The generalized gradient approximation (GGA)

LDA is expected to perform well for systems with a slowly varying density. Practically, such a condition is rarely satisfied. The first logical step to go beyond LDA is the use of more sophisticated exchange-correlation potentials where the exchange-correlation energy not only depends on the charge density at a particular point r, but also of the spatial variation of this electronic density at this point in order to take into account the non-homogeneity of the true electron density [29]. This can be done by adding gradient terms of the electron density to the exchange-correlation energy and its corresponding potential.

This has led to the generalized gradient approximation (GGA) which can be put in the general form:

$$E_{XC}^{GGA}[\rho] = \int g(\rho, g)|_{\substack{\rho=\rho(r) \\ g=\nabla\rho(r)}} d^3r \qquad (I.50)$$

Where g (ρ, g) is a function of the local density and density gradient. Function g is not unique and many different forms have been suggested because the electronic density gradient information can be included in many ways in GGA functional. The four most widely used GGAs are the forms proposed by Becke [30] (B88), Perdew et al. [31], Perdew, Burke and Enzerhof [32] (PBE) and that suggested by Perdew et al (PBESOL) [33].

Large number of test calculations showed that GGA functionals a noticeable improvement upon LDA in the description of atoms and solids [32]. Especially in systems where charge density varies rapidly, because GGA functional include more physical ingredients than the LDA functional but computationally it is more time consuming than LDA [34]. It underestimates the bulk modulus and zone center transverse optical phonon frequency of the solid [35,36], corrects the binding energy [37,36] and corrects or overcorrects the lattice constants compared to LDA [35,38-40]. However, the GGA approximation does not necessarily lead to better results than the LDA. There are several cases in which GGA gives worse results than LDA - for example, GGA sometimes overcorrects the results of LDA in ionic crystals where the lattice constants from LDA calculations agree well with the experimental data, but GGA will overestimate it. Nevertheless, LDA and GGA behave badly in materials where electrons tend to be localized and highly correlated such as transition metal oxides and rare earth elements and compounds.

References

[1] D. Landau and E. F. Lifshitz, *Quantum Mechanics Non-Relativistic Theory*, 3rd ed., Pergamon Press, Oxford, (1977).

[2] A. Messiah, *Quantum Mechanics. vol. 1*, North Holland Publishing Company: Amsterdam, (1964).

[3] M. Born, J. R. Oppenheimer, *Ann. d. Physik*. **84**, 457, (1927).

[4] D.R. Hartree, *Proc. Cambridge Phil. Soc*. **24**, 89 (1928).

[5] E. Kaxiras, *Atomic and Electronic Structure of Solids*, Cambridge University Press, Cambridge (2003).

[6] W. Pauli, *Zeitschrift für Physik* .**31**, 765 (1925).

[7] V. Fock, *Z. Phys*. **61**, 126 (1930).

[8] J. C. Slater, *Phys. Rev*. **35**, 509 (1930).

[9] F. Jensen, *Introduction to Computational Chemistry*, Chichester, Wiley, (1999).

[10] C. Pisany, R. Dovea, and C. Roetti, *Hartree-Fock Ab-initio Treatment of Crystalline Systems*, Springer, Berlin (1988).

[11] W. Kohn, A. D. Becke, and R. G. Parr, *J. Phys. Chem.* **100**, 12974 (1996).

[12] L. H. Thomas, *Proc. Cambridge Philos. Soc*. **23**, 542 (1927).

[13] E. Fermi, *Z. Phys*. **48**, 73 (1928).

[14] P. Hohenberg and W. Kohn, *Phys. Rev*. **136**, 864 (1964).

[15] W. Kohn and L. Sham, *J. Phys. Rev. A* **140,** 1133 (1965)

[16] J. Callaway, N. H. March, *Solid State Physics*, **38**, 135 (1984).

[17] M. Levy, *Phys. Rev. A* **26**, 1200 (1982).

[18] E. H. Lieb, *Density Functionals for Coulomb Systems, in Physics as Natural Philosophy: Essays in Honor of Laszlo Tisza on His 75th Birthday*, edited by A. Shimony and H. Feshbach, MIT Press, Cambridge, Mass., (1982),

[19] G. Vignale and M. Rasolt, *Phys. Rev. Lett*. **59**, 2360 (1987).

[20] G. Vignale and M. Rasolt, *Phys. Rev. B* **37**, 10685 (1988).

[21] N. D. Mermin, *Phys. Rev*. A **137**, 1441 (1965)

[22] R. M. Martin, *Electronic Structure Basic Theory and Practical Methods*," Cambridge University Press, Cambridge, (2004).

[23] M. Springborg and Y. Dong, *Metallic Chains / Chains of Metals*, Elsevier, Amsterdam, (2007).

[24] Philip L. Taylor & Olle Heinonen, *A Quantum Approach to Condensed Matter Physics*, Cambridge University Press (2002).

[25] D.M. Ceperley, B.J. Alder, *Phys. Rev. Lett*. **45**, 566 (1980).

[26] J. P. Perdew and A. Zunger, *Phys. Rev*. B **23**, 5048 (1981)

[27] D. S. Sholl and J. A. Steckel, *Density Functional Theory: A Practical Introduction*, John Wiley & Sons, New Jersey, (2009).

[28] J. P. Perdew, A. Ruzsinszky, L. A. Constantin, J. Sun, and G. I. Csonka, *J. Chem. Theory Comput*. **5**, 902 (2009)

[29] W. Koch and M. C. Holthausen, A Chemist's Guide to Density Functional Theory, Wiley—VCH, New York, (2000).

[30] A. D. Becke, Phys. Rev. A **38**, 3098 (1988).

[31] J. P. Perdew, J. A. Chevary, S. H. Vosko, K. A. Jackson, M. R. Pederson and C. Fiolhais, *Phys. Rev*. B **46**, 6671 (1992).

[32] J. P. Perdew, K. Burke, and M. Ernzerhof, *Phys. Rev. Lett*. **77**, 3865 (1996).

[33] J.P. Perdew, A. Ruzsinsky, G.I. Csonka, O.A. Vydrov, G.E. Scuseria, L.A. Constantin, X. Zhao, K. Burke, *Phys. Rev. Lett*. **100**, 136406 (2008).

[34] El-Barbary, *First principles characterisation of defects in irradiated graphitic materials*, Ph.D. thesis, University of Sussex, 2005

[35] C. Filippi, D.J. Singh and C.J. Umrigar, *Phys. Rev*. B **50**, 14947 (1994).

[36] A. D. Corso, A. Pasquarello, A. Baldereschi, and R. Car, *Phys. Rev*. B **53**, 1180 (1996).

[37] G. Ortiz, *Phys. Rev*. B **45**, 11328 (1992).

[38] A. Khein, D. J. Singh, and C. J. Umrigar, *Phys. Rev*. B **51**, 4105 (1995).

[39] Y. M. Juan and E. Kaxiras, *Phys. Rev*. B **48**, 14944 (1993).

[40] A. Garcia, C. Elsaesser, J. Zhu, S. Louie, and ML. Cohen, *Phys. Rev*. B **46**, 9829 (1992).

Chapter II
Pseudopotential Plane-Wave method

II.1 Introduction

In order to solve the Kohn-Sham equations, it is necessary to choose an appropriate base adapted to the studied system in order to develop the eigenstates of Kohn Sham and to express the different parts of the Hamiltonian. For the description of crystals, the set of plane wave is a good choice, because crystal lattices have periodic symmetry, which can be used to reduce the amount of atoms that must be accounted in the calculation. However, the plane wave become fast oscillation functions near the atomic nuclei, and therefore a large number of functions are needed to describe such oscillations. Nevertheless, using the pseudopotential approximation, we can reduce the size of the base set and thus reduce computational costs. The use of the plane wave basis with the pseudopotential constitutes the pseudopotential plane wave method.

In this chapter, we describe the expression of the Kohn-Sham equations in the plane wave basis, then, we will represent the pseudopotential approximation, followed by a practical methodology to solve the Kohn-Sham equations.

II .1 Crystal symmetry and Bloch's theorem

II .1.1 Periodic systems

A crystal is an ordered state of matter in which the positions of the nuclei (and consequently all properties) are repeated periodically in space. It is completely described in real space in terms of non-coplanar basis vectors $\vec{b}_1$, $\vec{b}_2$, $\vec{b}_3$ and the positions of atoms inside a primitive unit cell (PUC). The lattice vectors R are formed by all the possible combinations of primitive lattice vectors, multiplied by integers:

$$\vec{R} = n_1\vec{b}_1, +n_2\vec{b}_2 + n_3\vec{b}_3 \qquad \text{(II. 1)}$$

Where n_1, n_1 and $n_1$are integers.

A lattice formed by such a translational operation is called the simple Bravais lattice, and the parallelepiped defined by the three basis vectors $\vec{b}_1$, $\vec{b}_2$, $\vec{b}_3$ is the unit cell of the Bravais lattice (or primitive cell); its volume is:

$$\vec{V} = \vec{b}_1 \times (\vec{b}_2 \times \vec{b}_3) \qquad \text{(II. 2)}$$

There are infinite possible choices for the unit cell, the cell which is the most symmetric and compact is called the Wigner-Seitz unit cell.

Since the motion of electrons in a crystal is usually described in both real space and momentum space (or k-space), it is important to introduce the concepts of reciprocal lattice,

which is the inverse of the real lattice. In a reciprocal lattice a set of reciprocal basis vectors $\vec{b}^*_1, \vec{b}^*_2, \vec{b}^*_3$ can be defined in terms of the basis vectors $\vec{b}_1, \vec{b}_2, \vec{b}_3$ of a direct lattice. This is given by [1]:

$$\vec{b}^*_1 = \frac{2\pi(\vec{b}_2 \times \vec{b}_3)}{\vec{b}_1.(\vec{b}_2 \times \vec{b}_3)}, \quad \vec{b}^*_2 = \frac{2\pi(\vec{b}_3 \times \vec{b}_1)}{\vec{b}_2.(\vec{b}_3 \times \vec{b}_1)}, \quad \vec{b}^*_3 = \frac{2\pi(\vec{b}_1 \times \vec{b}_2)}{\vec{b}_3.(\vec{b}_1 \times \vec{b}_2)} \qquad \text{(II. 3)}$$

The primitive cell of the reciprocal space does not need to be a parallelepiped, in fact we can define the Wigner-Seitz cell of the reciprocal lattice, which is also known as the first Brillouin zone in reciprocal space.

In a perfect crystal, the Hamiltonian H of the Schrödinger equation of a system of particles is invariant under any translation operation T (n), as the effective potential has the same periodicity of the lattice and the derivative operator is invariant under the effect of translation operations [2].

II.1.2 Bloch's theorem

If we solve the Schrödinger equation for the periodic system, the solution must satisfy a fundamental property known as Bloch's theorem [3], which indicates that the eigenfunctions can be expressed by plane waves modulated by functions that have the same periodicity of the lattice. Using Bloch's theorem, the solutions of the Schrodinger equation for a periodic potential reads:

$$\psi_{n,k}(r) = \exp(ikr)\, u_{n,k}(r) \qquad \text{(II. 4)}$$

where $u_{n,k}(r)$ is a periodic wavefunction with $u_{n,k}(r) = u_{n,k}(r + R)$,R is any vector connecting equivalent Bravais lattice points, k is a reciprocal vector used to label the states and it can be always translated back to the first Brillouin zone, the subscript n is denoted as band index and distinguishes different eigen energy $\varepsilon_{n,k}$ for the same momentum k. The eigenvalues are also periodic functions in the reciprocal space, i.e.

$$\varepsilon_{n,k} = \varepsilon_{n,k+K} \qquad \text{(II. 5)}$$

This means that the Bloch's theorem reduces the number of electrons required for the calculation to those in the unit lattice, if the Hamiltonian of system is invariant under translation. The periodicity of $u_{n,k}(r)$ means that it can be expanded in terms of a special set of plane waves:

$$u_{n,k}(r) = \sum_G \tilde{u}_G \exp(iGr) \qquad \text{(II. 6)}$$

Where the summation is over all vectors defined by G:

$$\vec{G} = m_1\vec{b}^*_1 + m_2\vec{b}^*_2 + m_3\vec{b}^*_3 \qquad \text{(II. 7)}$$

Where m_1, m_2, m_3 are integers, and $\vec{b}_1^*$, $\vec{b}_2^*$, $\vec{b}_3^*$ are the reciprocal lattice vectors, and $\tilde{u}_G$ are the coefficients of expansion.

By combining the equations. (II.4) and (II.6), we can find that the single-particle wave functions $\psi_{n,k}(r)$,at each point k in the BZ of a given crystal, can be developed in a discrete set of plane waves:

$$\psi_{n,k}(r) = \exp(ikr)\, u_{n,k}(r) = \sum_G c_{nk}(G) \exp[\, i(k+G).r] \qquad \text{(II. 8)}$$

II.2 Expression of Kohn-Sham equations in the plane wave basis

Expansion of the electron wave functions in terms of plane waves allow the Kohn-Sham equations to take a particularly simple formulation in a reciprocal space [4, 5]. Substituting the electronic wavefunction expressed in terms of all plane waves equation (I.42) into the Kohn Sham equation (I.45) and integrating over r, gives the matrix eigenvalue equation:

$$\left[\sum_{G'} \frac{1}{2}|k+G|^2 \delta_{GG'} + V_{ext}(G-G') + V_{xc}(G-G') + V_H(G-G')\right] = \varepsilon_i C_{Gnk} \qquad \text{(II.9)}$$

In equation (II.9), the kinetic energy is diagonal, the other three terms on the left are the Fourier components of the external potentials, exchanges correlation and Hartree term respectively.

II .3 The cut-off energy

In principle, to describe exactly the electron wave function, the dimension of the plane-wave basis set should be infinite. However, the functions appearing in the equation. (II.8) have a simple interpretation as solutions of the Schrödinger equation: they are solutions with kinetic energy:

$$E = \frac{h^2}{2m}|k+G| \qquad \text{(II. 10)}$$

Typically, the plane wave functions with higher | G | have a higher kinetic energy and thus contribute less to the expansion of the wave function, because the coefficients $c_{nk}(G)$ associated with a plane wave of high kinetic energy are negligible compared to those associated with a plane wave of low kinetic energy [6].

Therefore, the size of the set of reciprocal lattice vectors can be truncated by placing an upper limit for the kinetic energy of the plane waves. This limit is called the cut-off energy such that only plane waves with a kinetic energy lower than E_{cut} are included in the expansion of Kohn-Sham functions. The infinite sum is then reduced to:

$$\psi_{n,k}(r) = \sum_{|G+k|<G_{cut}} c_{nk}(G) \exp[\, i(k+G).r] \qquad \text{(II. 11)}$$

Obviously, the value E_{cut} affects the accuracy of the calculations and depends strongly on the elements, which are present in the system under investigation. Simple convergence tests should be carefully performed in each case by varying the cut-off energy and establishing at what energy convergence is achieved. (i.e. increasing the cut-off energy does not affect the calculated energy of the system).

II.4 Sampling the Brillouin Zone

The computation of many physical quantities such as the total energy of a solid requires the knowledge of Bloch functions over infinite k points in BZ, because for each of k values exists a discrete spectrum of eigenvalues of the Kohn-Sham equation. Therefore, a finite selection of k points must be used in practice for the calculation. The electronic wave functions at k points that are very close together will be almost identical (it will not change much with small variations in k) [7]. Hence, it is possible to represent the electronic wave functions over a region of k space by the wave functions at a single k point. Thus removes the need for an infinite number of electrons and allows one to make calculations at the finite number of k points. By using the additional symmetries of the crystal, such as the rotations or reflections of the mirror, the number of points k required can be reduced, so that ψ can only be calculated at special points in the Brillouin zone and the integration can be conveniently confined in a smaller region of the BZ. The smallest possible part, that by employed all symmetries operations can be unfolded into the whole Brillouin zone is called the irreducible Brillouin zone (IBZ).

There are different methods for choosing special points in the BZ [8-10]. However, the Monkhorst-Pack approach is the most widely used [11]. The Monkhorst-Pack method is based on a representation of the integration on the BZ by a weighted sum over a number of special k-points. The error that appears in the calculations can be reduced by choosing a heavier set of k-points in the Brillouin zone.

II .5 Pseudopotential

II .5.1 The frozen core approximation

It is a well-known fact in chemistry that the core electrons, by opposition to the valence electrons, are tightly bounds to the nuclei and do not participate in the chemical bonding between atoms [12,13]. When the atoms are transferred from one chemical environment to another, the wave functions of the core electrons do not change significantly with the

environment of the parent atom, because their wave functions overlap only very slightly with the core electron wave functions from neighboring nucleus. For this reason, they do not determine most of the electronic and optical properties of materials. [14]. It is thus justified to consider the configuration of the core electrons within the solid to be "frozen" and equal to its form of the isolated atom. Therefore, it is possible to combine the potential due to the core electrons with the Coulomb potential of the nucleus to an ionic core potential. In this way, core electrons are removed from the problem and one can focus only on the valence electrons in the calculation, this is known as the frozen core approximation [15]. The error introduced by such an approximation is quite small but savings in the computational cost is enormous.

II .5.2 Concept of pseudopotentials

The atomic wave functions are eigenstates of the atomic Hamiltonian, they must all be mutually orthogonal, so that the valence wave function must oscillate rapidly and must has some nodes in the vicinity of the nucleus in order to maintain orthogonal to the core state. But ,it is difficult to develop the rapidly oscillating wave function with all of its radial nodes in a given basis set (e.g., Gaussian, plane waves, etc.), because an extremely large number of waves would be necessary to perform an all-electron calculation -a computationally demanding task, therefore, a further reduction of the basis set size is essential.

As the valence wave function is associated with bonding properties, a good description of valence wave function in core region is not necessary. It is therefore appropriate to attempt to replace the true potential, which includes the effects of the nucleus and the core electrons, by an effective pseudopotential acting only on valence electrons. As such, the rapid oscillations of the wave functions near the nuclei is replaced with a pseudo wave function. Pseudopotentials should be transferable between different chemical environments; ideally, a pseudopotential is constructed from an isolated atom of one element, but the resulting pseudopotential can be used for the same atomic species in another environment without further adjustment of the pseudopotential. This suggests that the pseudo-wave functions must be identical to the true valence wave functions in the region of the chemical bond (outside the ionic core region) where they overlap with other atoms [15] (see Figure II.1). An additional requirement for pseudopotentials is to be as smooth as possible in the core region [16, 17]. This is necessary to maintain the basis for the expansion of the wave functions as small as possible.

The use of pseudopotential method can reduce the size of the basis set necessary for calculations involving many atoms, therefore reduce the computational expense.

Pseudopotentials requiring high cut-off energies are called to be hard, while more computationally efficient pseudopotentials with low cut-off energies are soft.

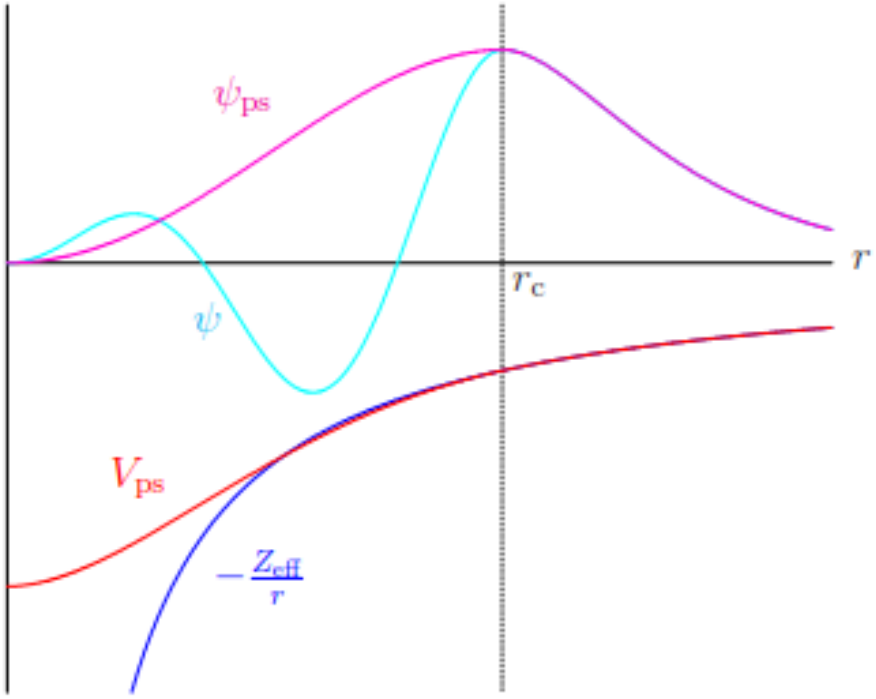

Fig. II.1. Schematic diagram of the relationship between all-electron and pseudopotentials and wave functions.

II 5.3 Ab initio Pseudopotentials

There is no single way to build a pseudopotential for a particular chemical element; there is an enormous freedom in constructing pseudopotentials [18-20].

In past, empirical pseudopotentials (they do not come from the first principles) constructed by fitting to the experimental data have been adopted [21, 22]. Although, these empirical pseudopotentials are simple to use, they lack a very important property, the transferability. They can be used for some specific environment but not in a different environment.

At present, there are many pseudopotentials that are constructed with non-empirical approaches. Pseudopotentials generated by calculations on atoms and are not fitted to experiments are called ab initio pseudopotentials. The ab initio pseudopotential method is now

a well-established tool in condensed matter physics, computational chemistry and material science.

The use of pseudopotentials dates back to Fermi's work in the 1930s to study high-lying atomic levels [23]. However, the most elegant way to present a non-empirical pseudopotential is due to Phillips and Kleinman [24, 25] who developed a rigorous formulation of the pseudopotential approach.

II.5.3.1 Method of Philips and Kleinman

To illustrate the pseudopotential idea suggested by Phillips and Kleinman, we distinguish between the states of the valence electrons $|\psi_v\rangle$ and the states of the core electrons$|\psi_c\rangle$ of a given Hamiltonian (for example the Fock operator in the Hartree-Fock theory or the Kohn-Sham operator in density-functional theory.)

The core electrons wave functions are defined by:

$$\hat{H}|\psi_c\rangle = \varepsilon_c|\psi_c\rangle \qquad (c = 1, N_c) \tag{II. 12}$$

The valence electron wave functions for this same Hamiltonian is given by,

$$\hat{H}|\psi_v\rangle = \varepsilon_v|\psi_v\rangle \qquad (v = 1, N_v) \tag{II. 13}$$

$|\psi_v\rangle$ has a number of radial nodes because it must be orthogonal to the core orbitals. Philips and Kleinman showed that one can construct a smooth valence wave function $|\hat{\psi}_v\rangle$, that is not orthogonal to the core state ($\langle\hat{\psi}_v|\psi_c\rangle \neq 0$), by combining the core wave functions $|\psi_c\rangle$ and the function of the real valence wave function $|\psi_v\rangle$ in the following way :

$$|\hat{\psi}_v\rangle = |\psi_v\rangle + \sum_{c=1}^{N_c} b_c|\psi_c\rangle \tag{II. 14}$$

b_c is some (yet) unknown constants, and $|\psi_c\rangle$ is the core wavefunctions.The constants b_c can be determined by using that the core wave functions are orthonormal, and that$|\psi_v\rangle$ is orthogonal to the core wavefunctions. We multiply Eq. (II. 14) by any of the core wavefunctions, $|\psi_{c0}\rangle$, and integrate, we obtain :

$$\langle\psi_{c0}|\hat{\psi}_v\rangle = \langle\psi_{c0}|\psi_v\rangle + \sum_c b_c \langle\psi_{c0}|\psi_c\rangle \tag{II. 15}$$

Where

$$\langle\psi_{c0}|\hat{\psi}_v\rangle = b_{c0} \tag{II. 16}$$

By using the fact that $|\psi_v\rangle$ and $|\psi_c\rangle$ are solutions of the Schrodinger equation with eigenvalues ε_v and ε_c, respectively, one easily obtains the following equation for$|\hat{\psi}_v\rangle$:

$$\left[\hat{H} + \sum_{c=1}^{N_c}(\varepsilon_v - \varepsilon_c)|\psi_c\rangle\langle\psi_c|\right]|\hat{\psi}_v\rangle = \varepsilon_v|\hat{\psi}_v\rangle \tag{II. 17}$$

$$\left[\hat{T} + \hat{V} + \sum_{c=1}^{N_c}(\varepsilon_v - \varepsilon_c)|\psi_c\rangle\langle\psi_c|\right]|\hat{\psi}_v\rangle = \varepsilon_v|\hat{\psi}_v\rangle \quad \text{(II. 18)}$$

The above result suggests to construct a pseudo-Hamiltonian:

$$\hat{H}_{Ps} = \hat{T} + \hat{V}_{ps} \quad \text{(II. 19)}$$

With a pseudopotential

$$V_{PS} = V + \sum_{c=1}^{N_c}(\varepsilon_v - \varepsilon_c)|\psi_c\rangle\langle\psi_c| \quad \text{(II. 20)}$$

So,

$$\hat{H}_{Ps}|\hat{\psi}_v\rangle = \varepsilon_v|\hat{\psi}_v\rangle \quad \text{(II. 21)}$$

This equation indicates that states $|\hat{\psi}_v\rangle$ satisfy a Schrodinger-like equation with an additional contribution, $\hat{V}_{ps}$ to the Hamiltonian.

Since $\hat{V}_{ps}$ is not a usual potential, it is called pseudopotential. i.e., a function depending on a position r, .It is important to note that the operator $\hat{V}_{ps}$is energy-dependent because it depends on ε_v, and it is nonlocal because it depends$|\psi_v\rangle$.

Since valence electron energies always lie above the core energies (i.e., $\varepsilon_v > \varepsilon_c$), the second term in Equation (II. 20)is always positive. Since $V(r)$ is attractive, the first term will be negative, which will be partially cancelled by the second term.

The pseudopotential acts differently on wave functions of different angular momentum, thereby expressing its energy dependence. The most general form of a pseudopotential of this kind is:

$$V_{ps}(r) = \sum_{\ell=0}^{\infty}\sum_{m=-\ell}^{\ell} V_\ell^{PS}(r)|\ell m\rangle\langle\ell m| = \sum_{\ell=0}^{\infty} V_\ell^{PS}(r)\,\hat{P}_\ell \quad \text{(II. 22)}$$

Where $|\ell m\rangle$ are the spherical harmonics $\langle r|\ell m\rangle = Y_{\ell m}(\theta,\phi)$, V_ℓ^{PS} is the pseudopotential corresponding to the angular component l , and the operator $\hat{P}_l = \sum_{m=-l}^{l}|\ell m\rangle\langle\ell m|$ is a projection operator onto the l th angular momentum subspace.

The meaning of the expression for V_ℓ^{PS} in Eq. (II. 22) is that when V_ℓ^{PS} operator acts on the electronic wave function, the projection operator $\hat{P}_l$ selects the different angular momentum components of the wave function, which are then multiplied by the corresponding pseudopotential V_ℓ^{PS}. Next, the contributions of all the angular momentums are added up to form the total pseudopotential contribution to the Hamiltonian matrix elements that enter Schrödinger equation.

Since V_ℓ^{PS}acts as a local operator in the radial coordinate that depends on ℓ, it can be called a angular-dependent or semi local pseudopotential. A local pseudopotential is a function only of the distance from the nucleus [26].

The work of Phillips and Kleinman first established the theoretical basis of the

pseudopotential method which can broadly be assigned into two categories: norm-conserving pseudopotentials and the ultra-soft pseudopotential.

II .5.3.2 Norm conserving pseudopotentials

II .5.3.2.1 Concept of Norm conserving pseudopotentials

A major step forward in the attempts to produce transferable first principles pseudopotentials came with the advent of norm conserving pseudopotentials by Hamann, Schlüter and Chiang [27] in 1979 and developed by Kleinman and Bylander [28]. Within this approximation, the all–electron and the pseudo wave function must have the same norm in the ionic core region delimited by a certain radius chosen called cut-off radius r_c to guarantee that both wave functions generate identical electron densities in the outside region. The pseudo and all-electron wave functions are identical outside the core radius but they are different inside the region of the ionic core delimited by the cut-off radius r_c. The charge conservation property of norm-conserving pseudopotentials simplifies the application of the pseudopotentials and makes them more accurate and transferable, they can be used to predict the physicochemical properties of an atom in a wide range of situations (volume, surface, etc.). However, the use of norm-conserving pseudopotentials is very expensive, due to the requirement of conservation of the norm below the r_c. They require large plane-wave basis sets or a large energy cut-off for elements with strongly localized orbitals such as the case of transition metals and rare earths, thus requiring much more computational effort.

II .5.3.2.2 The construction of the norm-conserving pseudopotential

The construction of a pseudopotential ('ab initio') is an inverse problem. However, there are important rules that help to solve the problem. We present here briefly the main stages of construction formulated first by Hamann et al [27] and exploited by Bachelet, Hamann and Schlüter (BHS) [29] who applied this methodology to all atoms from hydrogen to plutonium.

The following is the process of constructing the norm-conserving pseudopotential:

First, the real radial wave function $R_{n\ell}(r)$ of the atom is obtained by solving the radial equation of Kohn-Sham

$$\left[-\frac{1}{2r}\frac{\hbar^2}{m_e}\frac{d^2}{dr^2}r+\frac{\hbar^2}{2m_e}\frac{\ell(\ell+1)}{r^2}+v(r)\right]R_{n\ell}(r)=e_{n\ell}R_{n\ell}(r) \qquad (\text{II}.23)$$

Where

$$V(r)=-\frac{1}{r}+V_H(r)+V_{XC}(r) \qquad (\text{II}.24)$$

Here, $V_{XC}(r)$ is the exchange correlation potential and $V_H(r)$ is given by:

$$V_H(r) = \int \frac{\rho(r')}{|r-r'|} d^3r' \qquad \text{(II. 25)}$$

Where $\rho(r')$is the total electron density.

Once the true radial wave function $R_{n\ell}(r)$ is obtained, we choose a cut-off radius r_c (generally between the outermost node and the outermost extremum of the all-electron radial wave function) to construct a pseudo radial function $R_{n\ell}^{ps}(r)$satisfying five general criteria:

- The pseudowave function must be identical to the true valence wave function beyond the chosen cut-off radius:

  $R_{n\ell}^{ps}(r) = R_{n\ell}(r)$ pour $\quad r \geq r_c$) (II. 26)

- The pseudowave function $R_{n\ell}^{ps}(r)$ must not contain no nodes and be continuous at re, as well as its first and second derivatives. Since the pseudowave function is constructed only for valence electrons, we omit the principal quantum number n.
- The normalized atomic radial pseudowave function $R_{n\ell}^{ps}(r)$ and normalized radial true wave function $R_\ell(r)$ must be equal beyond a suitably chosen cut-off radius r_c

  $\left|R_{n\ell}^{ps}(r)\right|^2 = |R_{n\ell}(r)|^2$ pour $r \geq r_c$ (II. 27)

- The eigenvalues of pseudowave function must be equal to the true eigenvalues.
- The charge enclosed within r_c for the pseudowave function and true wave function must be equal, that is

  $$\int_0^{r_c} \left|R_{n\ell}^{ps}(r)\right|^2 r^2 dr = \int_0^{rc} |R_{n\ell}(r)|^2 r^2 dr \qquad \text{(II. 28)}$$

The last condition is commonly referred to as the norm-conservation condition and if a pseudopotential meets this condition, it is called a "norm-conserving pseudopotential" (NCPP). Note that a pseudowave function fulfilling these conditions can be constructed arbitrarily in many ways. This freedom is further exploited to produce a smooth pseudopotential. Once a particular pseudo-wave function is created, the screened pseudopotential can be recovered by inverting the radial Schrodinger equation (II.24):

$$\mathrm{V}_{\ell \mathrm{Sc}}^{\mathrm{Ps}}(\mathrm{r}) = \mathrm{e}_{\mathrm{n}\ell} - \frac{\ell(\ell+1)}{2\mathrm{r}^2} + \frac{1}{2\mathrm{r}\mathrm{R}_\ell^{\mathrm{PS}}} \frac{\mathrm{d}^2}{\mathrm{dr}^2}\left[\mathrm{r}\mathrm{R}_\ell^{\mathrm{PS}}(\mathrm{r})\right] \qquad \text{(II. 29)}$$

We call the resulting pseudopotential $V_{\ell Sc}^{Ps}(r)$ screened, because it still includes the potential due to the nucleus and all electrons, not just the core electrons. The screened pseudopotential $V_{\ell Sc}^{Ps}(r)$thus obtained lacks transferability as the screening from the valence electrons depends

strongly on the environment in which they are placed. To improve the transferability and generate a pseudopotential "ionic" (not screened) independent of the chemical environment, the interaction among the valence electrons (and their self-interaction) is removed from the screened PP by the so-called unscreening procedure. This is achieved by subtracting the screening Hartree and exchange–correlation potential, calculated solely by the pseudo valence orbitals (or rather their densities), from the screened pseudopotential.

By subtracting the effect of the valence electrons, one obtains an (unscreened) 'ionic' pseudopotential that does not depend on the chemical environment and, it should be transferable from the atom to a molecular state or to a solid state or liquid state. The ionic pseudopotential we are looking for is given by:

$$V_\ell^{PS}(r) = V_{\ell,sc}^{PS}(r) - \int dr' \frac{\rho_v^{PS}(r')}{|r-r'|} - V_{XC}[\rho_v^{PS}(r)] \qquad (II.30)$$

With

$$\rho_v^{PS}(r) = \sum_{\ell m}^{occ} \left| r R_\ell^{PS}(r) \right|^2 \qquad (II.31)$$

When such ionic potential is placed in a different environment, $V_H(r)$ and Vxc(r) are recalculated for that environment and again added to the potential. Note that this does not guarantee that the pseudopotential is transferable to any environment. It can be used only in an environment in which eigenvalues do not change significantly from the eigenvalues used in its construction. The property that makes this energy range wider is loosely called smoothness, that is, the smoother the pseudopotential, the weaker the energy dependence.

The norm-conserving pseudopotentials, constructed from equation (II.30), have a general semi-local form, because although the potentials are local in r, they depend in a non-local way on the angular variables. Through the orbital moment, each component of the angular momentum of the wave function sees a different potential [30]. The ionic pseudopotential can be expressed as follows [31]:

$$V^{PS} = \sum_{\ell=0}^{\infty} V_\ell^{PS} \hat{P}_\ell \qquad (II.32)$$

$\hat{P}_\ell$ is the operator defined in equation (II.21).

In general, we can express the non-local pseudopotential in semi-local form [26]:

$$\begin{aligned} V^{PS}(r) &= \sum_{\ell=0}^{\infty} V_{loc}^{PS}(r)\hat{P}_\ell + \sum_{\ell=0}^{\ell max} \left[V_\ell^{PS}(r) - V_{loc}^{PS}(r) \right] \hat{P}_\ell \\ &= \sum_{\ell=0}^{\infty} V_{loc}^{PS}(r)\hat{P}_\ell + \sum_{\ell=0}^{\ell max} \left[\Delta V_\ell^{PS}(r) \right] \hat{P}_\ell \end{aligned} \qquad (II.33)$$

With

$$\Delta V_\ell^{PS}(r) = V_\ell^{PS}(r) - V_{loc}^{PS}(r) \qquad (II.34)$$

Here $V_{loc}^{PS}(r)$and $\Delta V_{\ell}^{PS}(r)$ are the local and semi-local potentials respectively. The semi-local potential in equation (II.34) can be transformed into a completely non-local form using a general form suggested by Kleinman-Bylander (KB) [28] as:

$$V_{PP}^{KB} = V_{loc}^{PS} + \sum_{l,m} \frac{|\Delta V_{\ell}^{PS} \psi_{lm}^{PS}\rangle\langle\psi_{lm}^{PS} \Delta V_{\ell}^{PS}|}{\langle\psi_{lm}^{PS}|\Delta V_{\ell}^{PS}|\psi_{lm}^{PS}\rangle} \quad (II.35)$$

Where $\psi_{lm}^{PS}$is a proper state of the atomic pseudo-Hamiltonian. The operator V_{PP}^{KB}acts on the reference state identically to the original semi-local operator $V^{PS}(r)$,so that it is conceptually well justified, but now the number of projections that must be made varies only linearly with the number of basic states, whereas for semi-local forms, this number varies quadratically. This separable form can be seen as a "correction" to the local pseudopotential in the core region.

II .5.3.3 Vanderbilt Pseudopotential (Ultrasoft)

II .5.3.3.1 Concept of Vanderbilt Pseudopotential (Ultrasoft)

The " norm conserving pseudopotentials " approach has been extended by David Vanderbilt [32], by creating ultra-soft pseudopotentials. In this approximation, Vanderbilt [32] showed that then much smoother, but still highly transferable, non-norm-conserving pseudopotentials can be obtained by relaxing the norm-conserving constraint, which is the main factor responsible for the hardness of the norm conserving pseudopotentials. The only restriction remaining is, then, the matching of the pseudo and the all-electron functions for r ≥ rc, and this gives the possibility to choose a much larger value for r_c. Consequently, the kinetic energy is reduced, the valence electrons experience a smoother potential and the number of plane waves required for its description decreases. It is for this reason that Vanderbilt ultra-soft pseudopotentials are amongst the most widely used in the condensed matter community. Pseudopotentials can be made softer by moving the cut-off radius outward, however, there is an upper bound to the cut-off radius, if it is increased beyond this bound, the transferability of the pseudopotential reduces. The relaxation of the norm-conservation constraint causes a charge-density deficit between the pseudo wave function and the exact one that should be taken into account in the generation of the ultrasoft pseudopotential. This can be done by dividing the pseudo wave functions into two parts: Ultrasoft valence wave function that do not fulfil the norm conservation criteria plus, a core augmentation charge functions which are defined as the charge density difference between the all-electron and pseudo wave functions and are strictly localized in the core region.

$$Q_{nm}(r) = \psi_n^*(r)\psi_m(r) - \psi_n^{pp*}\psi_m^{pp} \quad (II.36)$$

Therefore, the norm-conservation will be satisfied when the $\mathrm{Q_{nm}(r)} = 0$.

II .5.3.3.2 The construction of ultrasoft potentials

The generation of ultrasoft potentials start out in the same way as norm-conserving pseudopotentials. For a given species, the atomic Kohn-Sham system is solved self-consistently, resulting the screened all-electron potential, VAE. Then for each angular momentum channel, a few energy values, τ are chosen (τ =number of such energies, usually max 3). For the V_{AE} already obtained, the Schrödinger equation is found

$$[T + V_{AE}]|\psi_n\rangle = \varepsilon_n|\psi_n\rangle \qquad \text{(II. 37)}$$

Here n is a composite index holding l for the angular momentum quantum number, m for the projection and τ. $n = \{\tau\ell m\}$.

Next, we choose three cut-off radii:

1. A smooth local (ℓ-independent) potential is created which matches V_{AE} after the radius r_c^{loc}.
2. A second cut-off radius r_{cl} , is chosen for each angular momentum channel and a pseudofunction, $\psi_{\mathrm{n}}^{\mathrm{pp}}$ is constructed which matches the real wave function $|\psi_n\rangle$ at r_{cl}.
3. Finally a diagnostic radius R is chosen such that it is slightly greater than the maximum of all radius r_c^{loc} and r_{cl}, so that all the quantities of PS and AE agree beyond R_c.

Then a smooth pseudofunction wave is determined for each angular momentum only with the constraint that it corresponds to the real wave functions outside the chosen cut-off radius r_{cl}.

The Kohn-Sham equations are then inverted to obtain the total effective V_{KS}^{PP} pseudopotential satisfying the following equations:

$$\left(\hat{T} + V_{eff}^{ps}\right)\psi_n^{pp} = \varepsilon_n\psi_n^{pp} \qquad \text{(II. 38)}$$

The total effective pseudopotential is then separated into a local and non-local contribution,

$$V_{KS}^{PP} = V_L + V_{NL} \qquad \text{(II. 39)}$$

The local potential V_L is chosen to be smooth, this potential agrees with the all-electron potential beyond cut-off radii chosen rc. By inserting the equation (II.40) in the equation (II.39), we can construct for each wave pseudofunction the following orbital [33]:

$$|\chi_n\rangle = \left[\varepsilon_n - T - \hat{V}_L\right]\left|\psi_n^{pp}(r)\right\rangle \qquad \text{(II. 40)}$$

The orbitals $|\chi_n\rangle$ are local and disappear beyond R where $V_{lo} = V_{AE}$ and $\psi_n^{PP} = \psi_n$Then, an auxiliary matrix of interior products is determined

$$(B^{-1})_{mn} = \langle\psi_n^{pp}|\chi_m\rangle \qquad \text{(II. 41)}$$

The projectors needed to define the non-local part of the potential are defined by:

$$|\beta_n\rangle = \sum_n|\chi_n\rangle\langle\chi_m|\psi_n^{pp}\rangle = \sum_n(B^{-1})_{mn}|\chi_m\rangle \qquad \text{(II. 42)}$$

The total non-local operator is then rewritten as:

$$\hat{V}_{NL} = \sum_{n,m} B_{nm} |\beta_n\rangle\langle\beta_m| \quad \text{(II. 43)}$$

Provided that the norm-conserving constraint of the pseudo-wave function is respected. The norm-conservation will be satisfied when:

$$\mathrm{Q_{nm}(r)} = \psi_{\mathrm{n}}^{*}(\mathrm{r})\psi_m(\mathrm{r}) - \psi_{\mathrm{n}}^{\mathrm{pp}*}\psi_{\mathrm{m}}^{\mathrm{pp}} = 0 \quad \text{(II. 44)}$$

We note that for the particular case where a single reference energy is chosen by angular momentum, the equation (II.42) simply returns to the Kleinman-Bylander form of the separable non-local potential [33]. Vanderbilt has shown that the norm-conserving constraint of equation (II.44) can be abandoned by introducing a generalized Hermitian overlap operator S:

$$S = 1 + \sum_{nm} q_{nm} |\beta_n\rangle\langle\beta_m| \quad \text{(II. 45)}$$

So that the orthonormality condition to satisfy in the solution of the KS equations is:

$$\langle\psi_n|S|\psi_m\rangle = \delta_{nm} \quad \text{(II. 46)}$$

In the expression (III.45) $q_{nm}$is the integral of the augmentation function $Q_{nm}(r)$ over the sphere defined by r_c:

$$q_{nm} = \int dr\, Q_{nm}(r) \quad \text{(II. 47)}$$

The new non-local operator V_{NL} becomes:

$$V_{NL} = \sum_{nm} D_{nm} |\beta_n\rangle\langle\beta_m| \quad \text{(II. 48)}$$

Where the new coefficients are:

$$D_{nm} = \mathrm{B}_{nm} + \varepsilon_m q_{nm} \quad \text{(II. 49)}$$

With all these descriptions, we can verify that the pseudo functions obey the equation

$$\left(\hat{T} + V_{loc} + \sum_{nm} D_{nm} |\beta_n\rangle\langle\beta_m|\right)\left|\psi_n^{pp}\right\rangle = \varepsilon_i(1 + \sum_{nm} q_{nm} |\beta_n\rangle\langle\beta_m|)\left|\psi_n^{pp}\right\rangle)$$

$$\left(\hat{T} + V_{loc} + \sum_{nm} D_{nm} |\beta_n\rangle\langle\beta_m|\right)\left|\psi_n^{pp}\right\rangle = \varepsilon_i S\left|\psi_n^{pp}\right\rangle \quad \text{(II. 50)}$$

It can be verified that the pseudopotentials ultrasoft generated with the above steps have excellent transferability; this means that the pseudo-wave functions and their logarithmic derivatives correspond to each reference energy and for small variations around it. To compensate for the charge deficit, the valence charge density is defined as

$$\rho(r) = \sum_n \left[\left|\psi_n^{ps}(r)\right|^2 + \sum_{i,j} Q_{ji}(r)\left\langle\psi_n^{ps}\middle|\beta_i\right\rangle\left\langle\beta_j\middle|\psi_n^{ps}\right\rangle\right] \quad \text{(II. 51)}$$

II .6 Resolution of Kohn-Sham equations

In order to set up and solve the Kohn–Sham equations, we need to define both the Hartree operator V_H and the exchange-correlation operator *Vxc* which depend on the density $\rho(r)$ .But to construct the electron density, we must know the single-electron wave functions,

and to find these wave functions we must solve the Kohn–Sham equations .Thus means the estimated solution of the Kohn-Sham problem must be known before it can be solved, so an iterative procedure is needed to escape from this paradox (See Figure II.2) . The Kohn-Sham equations of the system can be constructed for a trial electron density and for a given set of atomic coordinates. The geometries of the system for density functional calculation are constructed using experimental data such as bulk lattice constants, previous first principle calculations or semi-empirical methods, or from intuition. Once trial electron density and is defined, the Poisson's equation is constructed and solved in order to obtain the electrostatic Coulomb potential. Subsequently explicit form of the exchange-correlation potential is used and the exchange correlation operator is constructed. All these terms are added together to give the full Hamiltonian of equation (I.42)

Following standard mathematical techniques for solving eigenvalue problems, one can expand the unknown solutions $\psi_i(r)$ of the equation ((I.42)) for each k-point in a set of known functions, $\phi_j(r)$, with unknown linear coefficients, c_{ij},

$$\psi_i(r) = \sum_j c_{ij}\phi_j(r) \qquad (II.52)$$

There are many possible choices that could be made for the basis set, although Gaussians 25 have dominated the molecular community while plane waves have been the de facto standard for solid-state physics. In principle, $\phi_j(r)$ has an infinite dimension, i.e., but in practice one works with a limited set of basis functions that can generate a function that is 'close' to $\phi_j(r)$by using the technique discussed in section (II.4).

The coefficients that determine how much these functions contribute to the development of the Kohn-Sham function are found by constructing the energy functional (i.e. the expectation value of the Hamiltonian) and applying the Variational principle This transforms the partial differential equation to a discrete matrix problem that can then be solved:

$$\sum\left[\langle\phi_{ik}|H|\phi_{jk}\rangle - \varepsilon_{nk}\langle\phi_{ik}|\phi_{jk}\rangle\right]c_{ink} = 0$$

$$\sum\left[H_{ij} - \varepsilon_{nk}\,S_{ij}\right]c_{ink} = 0 \qquad (II.53)$$

where

$$H_{ij} = \langle\phi_{ik}|H|\phi_{jk}\rangle \qquad (II.54)$$

And

$$S_{ij} = \langle\phi_{jk}|\phi_{ik}\rangle \qquad (II.55)$$

Where H_{ij} is the matrix elements of the Kohn-Sham Hamiltonian in the basis states, and S_{ij} is the overlap matrix elements.

The diagonalization of the matrix (II. 53) at each k point produces a set of eigenvalues of a particle and the variational coefficients of expansion corresponding to each eigenvalue. The initial wave functions at each k-point in the irreducible wedge of the Brillouin zone could in principle be obtained by using the expansion coefficients. The occupation of each state is obtained by using Fermi-Dirac statistics. This indicates that the eigenvalues are generated with increasing energy and all states are filled until the total number of electrons of the system is exhausted.

The electron density at a specific point k is thus:

$$\rho^k(r) = \sum_{i=1}^{N} \left|\phi_i^k\right|^2 \qquad \text{(II. 56)}$$

Therefore, the new total electron density ("output") can be calculated via the summation of the densities at the sampled k-points,

$$\rho(r) = \frac{\Omega}{(2\pi)^3} \sum_{k}^{1^{eme}Bz} \rho^k(r)\, \Delta k \qquad \text{(II. 57)}$$

Where Δk is the k-point sampling spacing which could be manually determined. It is easy to see that the smaller Δk is selected, the more accurate the calculation of ρ (r) would be, , but as the number of electrons in the system increases, the computational cost will also increase, making almost impossible to solve systems with more than a few electrons. The constructed electron density is called the output electron density. If the output electron density is not equal to the input one, it will be used as an input and this process is repeated several times until the new-evaluated electron density can be equated to the old density. This is known as the self-consistent field cycle SCF. In practice, one iterates sufficiently long until the residual difference between the input and output densities does not cause any significant errors in the total energy or other properties of interest. The found electron density also corresponds to the ground state density, since this is the only density that can be correctly solved from the Kohn-Sham equation.

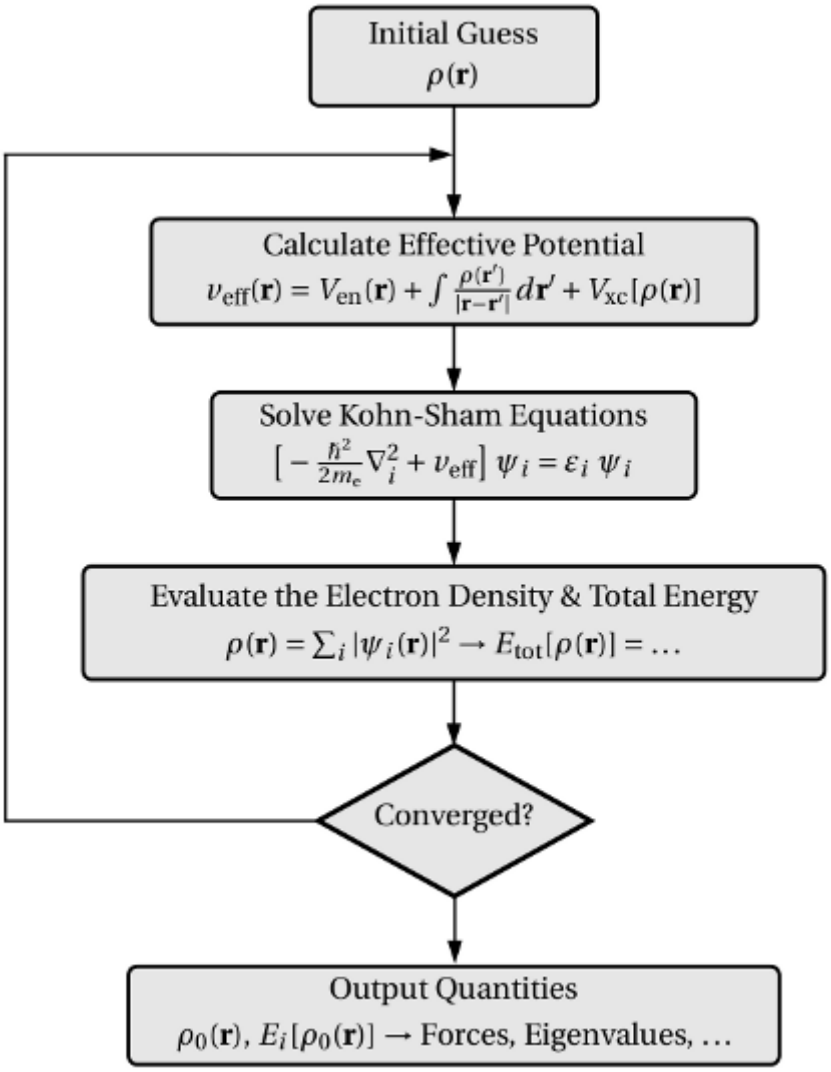

Fig. II.2. A flow chart of a typical DFT calculation within the Kohn Sham method.

References

[1] E. Kaxiras, Atomic and Electronic Structure of Solids, Cambridge University Press, Cambridge (2003).

[2] N.W. Ashcroft, N.D. Mermin: *Solid State Physics*, Holt Rinehart and Winston, New York (1976).

[3] F. Bloch, *Z. Physik* **52**, 555 (1928).

[4] M. C. Payne, M. P. Teter, D. C. Allan, T. A. Arias, and J. D. Joannopoulos, *Rev. Mod. Phys.* **64**, 1045 (1992).

[5] J. Ihm, A. Zunger, M.L. Cohen, *J. Phys.* C **12**, 4409 (1979).

[6] D. S. Sholl and J. A. Steckel, *Density Functional Theory: A Practical Introduction*, John Wiley & Sons, Hoboken, New Jersey (2009).

[7] L. P. Bouckaert, R. Smoluchowski, and E. Wigner. *Phys. Rev.* **50**, 58 (1936).

[8] D. J. Chadi and M. L. Cohen, *Phys. Rev.* B **8**, 5747 (1973).

[9] J. D. Joannopoulos and M. L. Cohen, *J. Phys.* C **6**, 1572 (1973).

[10] R.A. Evarestov and V.P. Smirnov, *Phys. Status Solidi* **119**, 9 (1983).

[11] H. J. Monkhorst and J. D. Pack, *Phys. Rev*. B **13**, 5188 (1976).

[12] R. M. Martin, "*Electronic Structure Basic Theory and Practical Methods*," Cambridge University Press, Cambridge, (2004).

[13] W. E. Pickett, Comput. *Phys. Rep*. **9**, 115 (1989).

[14] U. von Barth and C. D. Gelatt, *Phys. Rev.* B **21**, 2222 (1980).

[15] S. Goedecker and K. Maschke, *Phys. Rev.* A **45**, 88 (1992).

[16] V. Heine. *The pseudopotential concept. In Solid State Physics, Vol. 24*, Academic Press, New York (1970).

[17] W. E. Pickett, *Comp. Phys. Rep*. **9**, 115 (1989).

[18] M. L. Cohen and V. Heine. *The fitting of pseudopotentials to experimental data and their subsequent application, volume 24 of Solid State Physics.* Academic Press, New York, (1970).

[19] M.L. Cohen, J.R. Chelikowsky, *Electronic Structure and Optical Properties of Semiconductors*, Springer, Berlin, (1988).

[20] W. A. Harrison, "*Pseudopotentials in the Theory of Metals,* Benjamin, New York, (1966).

[21] B. J. Austin, V. Heine and L. J. Sham, *Phys. Rev*. **127**, 276 (1962).

[22] R.W. Shaw, Jr. and W.A. Harrison, *Phys. Rev*. **163**, 604 (1967).

[23] E. Fermi, *Nuovo Cimento* **11**, 157 (1934).

[24] J. C. Phillips, *Phys. Rev*. 112, 685 (1958).

[25J. C. Phillips and L. Kleinman, *Phys. Rev*. **116**, 287 (1959).

[26] J. Kohanoff, *Electronic structure calculations for solids and molecules: theory and computational methods*, Cambridge University Press, New York (2006).

[27] D. H. Hamann, M. Schlüter, and C. Chiang, *Phys. Rev. Lett*. **43**, 1494 (1979).

[28] L. Kleinman and D. M. Bylander, *Phys. Rev. Lett*. 48, 1425 (1982).

[29] G. B. Bachelet, D. R. Hamann, and M. Schlüter, *Phys. Rev*. B **26**, 4199 (1982).

[30] N. Troullier and J. L. Martins, *Phys. Rev*. B **43**, 1993 (1991)

[31] X. Gonze, R. Stumpf, and M. Scheffler, *Phys. Rev*. B **44**, 8503 (1991).

[32] D. Vanderbilt, *Phys. Rev*. B **41**, 7892 (1990).

[33] G. Kresse and J. Hafner, *J. Phys. Condens. Matter* **6,** 8245 (1994)

CHAPTER III

RESULTS AND DISCUSSIONS

III.1. Computational details

In order to benefit of the advantages of available computational methods, two complementary first-principles approaches in the framework of density functional theory (DFT) were used to perform a complete investigation of the structural, electronic and optical properties of Ag-based oxides LiAgO and NaAgO.

We have employed the first-principles pseudopotential plane-wave (PP-PW) method as implemented in the Cambridge Serial Total Energy Package (CASTEP) code [1] to determine the structural parameters. A new version of the generalized gradient approximation (GGA), namely the GGA-PBEsol [2], which has been developed specifically to improve the description of the exchange-correlation in solids, was used. Interactions of the valence electrons with the nucleus and frozen core electrons were modelled using Vanderbilt ultrasoft pseudopotentials [3]. The Li:$1s^2 2s^1$, O: $2s^2 2p^4$, Ag: $4d^{10} 5s^1$ and Na: $2s^2 2p^6 3s^1$ electrons were treated as valence states. Valence electronic wave functions were expanded in a plane-wave basis set truncated at maximum plane-wave energy (the cut-off energy) of 400 eV. The Brillouin zone (BZ) was sampled on a $6 \times 6 \times 3$ Monkhorst–Pack special k-mesh [4]. The self-consistent calculations were considered to converge when the difference in the total energy was within 5.0×10^{-7} eV/atom. Very careful step analysis is done to ensure convergence of the total energy, lattice parameters and optical properties in terms of the variational cut-off energy and number of k-points in the Brillouin zone. We have verified that further increase in the energy cut-off and k-point number did not lead to any noticeable changes in the total energy. We have also experimented with the basis set cut-off and number of k-points that at the equilibrium volume the cut-off energy of 400 eV and $6 \times 6 \times 3$ Monkhorst–Pack special k-mesh were sufficient in the sense that the predicted lattice parameters did not change noticeably when we increased the number of basis functions and k-point number. For optical properties, since the imaginary part of the dielectric function is usually calculated first, we choose it as a reference for the assessment of convergence. In optical calculations, a $16 \times 16 \times 9$ Monkhorst–Pack k-points sampling is found to be enough to get convergence value.

The geometry optimization of all free lattice parameters and internal coordinates was determined using the Broyden–Fletcher–Goldfarb–Shanno minimization technique [BFGS] [5], which is known to provide a fast way to find the lowest energy structure. The optimization was performed until the forces on the atoms were less than 0.01 eV/A, all the

stress components were less than 0.02 GPa and the tolerance in the self-consistent field (SCF) calculations was 5.0×10^{-7} eV/atom.

III.2. Results and discussion

III.2.1 Structural properties

Noncentrosymmetric (NCS) oxide materials with chemical formula BAgO (B = Li and Na) have tetragonal structure with space group $I4/mmm$ ($No.139$ in the international X-ray tables) [6]. The unit cell contains two chemical formula units (Z = 4). The atomic positions for the Ag, O and alkaline metal B atoms are respectively 8h (x_{Ag},x_{Ag},0), 8i (x_O,0,0) and 8j(0.5,y_B,0), where x_{Ag}, x_O and y_B are the so-called internal coordinates for the indicated atoms. Therefore, the crystalline structure of the considered compounds is characterized by five parameters not fixed by the symmetry group: the two lattice constants, a and c, and three internal coordinates, x_{Ag}, x_O and y_B. We optimized lattice parameters and internal coordinates, using the BFGS method, in order to perform calculations of the elastic properties of the compounds. The ground state structure parameters of the tetragonal BAgO materials are determined from geometry at $P=0GPa$, are given in Table 1 together with the available experimental [6] and theoretical results [7] for comparison. The obtained optimized lattice parameters, including the lattice constants, a_0 and c_0, and the internal parameters, x_{Ag}, x_O and y_B, for the three considered compounds are in good agreement with the existing experimental data [6]. Both lattice constants a and c are obtained within less than 1.5% deviation, in the worst case, from experimental values. This illustrates the level of accuracy that can be achieved in the modern DFT calculations. The error in the internal coordinates x_{Ag}, x_O and y_B is also small. As can be seen from Table 1, the a_0 and c_0 values of the BAgO compounds increase in the following sequence: { a_0 and c_0 }(LiAgO) < { a_0 and c_0 }(NaAgO). Since Ag and O atoms are the same in the two compounds, this result can be easily explained by considering the atomic radii R of Li and Na, which belong to the same column of the periodic table: R(Li) = 2.05 Å and R(Na)=2.23 Å; the larger size of B atom forces the system to have larger lattice constants.

To investigate the response of the BAgO (B = Li, Na) materials to an external pressure, a hydrostatic compression was applied to the unit cell in a 0–20 GPa pressure range with steps of 5 GPa. At each pressure a complete optimization of the structural parameters was performed. In Fig. 1, we plot the relative changes in the lattice constants, a/a_0 and c/c_0, versus applied hydrostatic pressure P. The symbols indicate the ab initio results for the given pressures. These data can be fitted by the following quadratic least squares fits

$(X/X0 = 1 + \alpha P + \beta P^2)$:

$$\text{LiAgO}\begin{cases}\dfrac{a}{a_0} = 1 - 0.0033p + 4.565 \times 10^{-5}p^2 \\ \dfrac{c}{c_0} = 1 - 0.0057p + 8.407 \times 10^{-5}p^2\end{cases}$$

$$\text{NaAgO}\begin{cases}\dfrac{a}{a_0} = 1 - 0.0051p + 6.878 \times 10^{-5}p^2 \\ \dfrac{c}{c_0} = 1 - 0.0072p + 15.447 \times 10^{-5}p^2\end{cases}$$

Table 1: Optimized lattice parameters (a_0 and c_0, in Å), internal coordinates (y_A, x_{Ag} and x_O), bulk modulus (B_0, in GPa), bulk modulus pressure derivative (B') at zero pressure for the LiAgO and NaAgO materials. Existing experimental and theoretical data are shown for comparison. B_0 and B' were obtained from the Birch EOS.

Parameter	Materials					
	LiAgO			**NaAgO**		
	Present	Expt.	Othe.	Present	Expt.	Othe.
a (Å)	9.1761	//	//	9.4292	9.520[b,c]	9.670[a]
c (Å)	3.8164	//	//	4.6551	4.617[b,c]	4.670[a]
c/a	0.4159	//	//	0.4937	0.483[b,c]	0.486a
y_B	0.1387	//	//	0.1619	0.1595	//
x_{Ag}	0.1624	//	//	0.1581	0.1558	//
x_O	0.3226	//	//	0.3107	0.3068	//
B_0	71.342	//	//	47.187	//	//
B'	4.7917	//	//	5.2806	//	//

From Fig. 1, one can note that the shrinkage degree along the *c* axis is practically the same for the two studied materials; this means that all these materials have practically the same stiffness against stress applied along the *c* axis. However, the compressibility along the *a* axis increases from LiAgO to NaAgO. The compressibility along the c axis is greater than that along the *a* axis in LiAgO and NaAgO. These results indicate that LiAgO and NaAgO are stiffer for stresses applied along the *a* axis than those applied along the *c* axis for all considered pressure range. One can state that these four compounds have practically the same

average bonding strength along the *c* axis, whereas the average bonding strength along the *a* axis decreases with the increase of the atomic number Z of the B (B = Li, Na) atom.

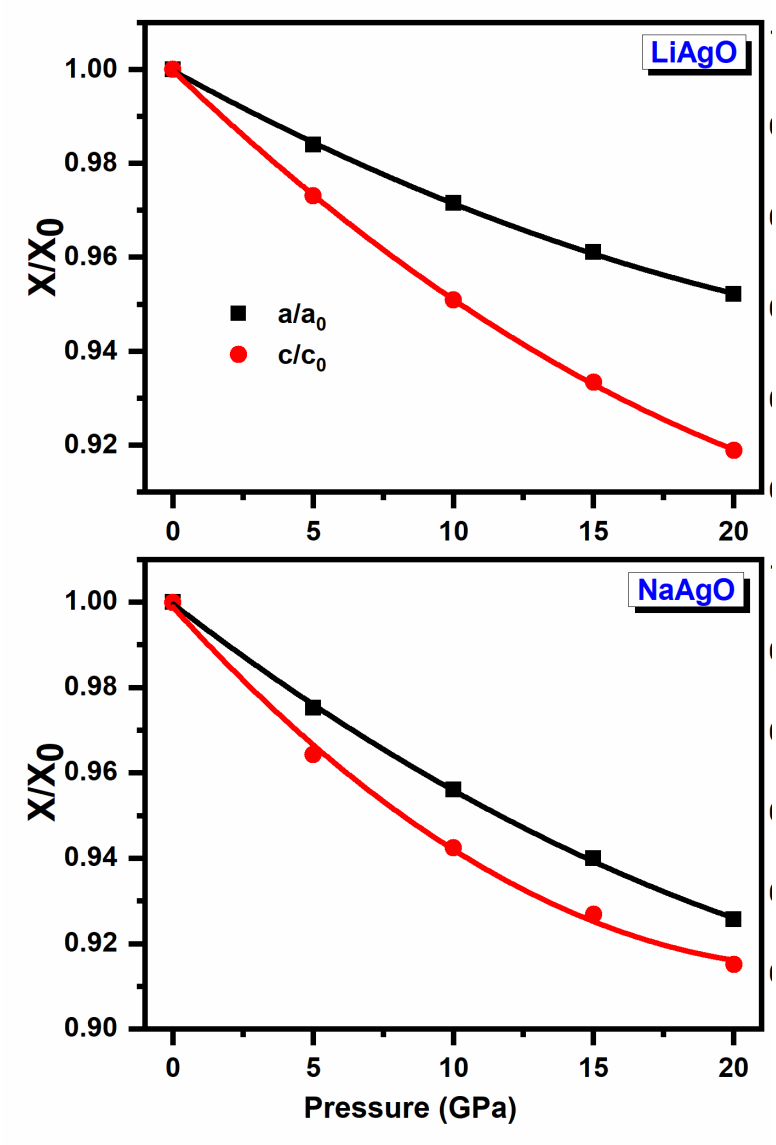

Fig. 1. Pressure dependence of the relative variations of the lattice constants *a* and *c* for the LiAgO and NaAgO materials. The ‘‘0’’ subscript denotes the lattice constants at zero pressure.

The calculated pressure dependence primitive-cell volumes were used to construct the equation of state (EOS) *P(V)* as shown in Fig. 2. From the Pressure–Volume data, fitted to the third-order Birch equation of state [8] (solid lines in Fig. 2), we obtain the bulk modulus at zero pressure B_0 and its pressure derivative *B'*. These are listed in Table 1. Our obtained bulk modulus values, using the GGA-PBE, are slightly smaller than the ones reported in Ref. [7]; this slight deviation could be attributed to the use of the LDA approach in Ref. [7], which is known to overestimate the bulk modulus value compared to the one obtained using the GGA

approach. We did not find experimental results for B_0 and B' in the literature to confirm these theoretical results. The BAgO bulk modulus values decrease in the following sequence: {B_0}(LiAgO) > {B_0}(NaAgO), i.e. in the reverse order compared to the {a_0 and c_0} case; this is in agreement with the well-known relationship between B_0 and the lattice constants: $B_0 \propto V_0^{-1}$, where V_0 is the primitive-cell volume.

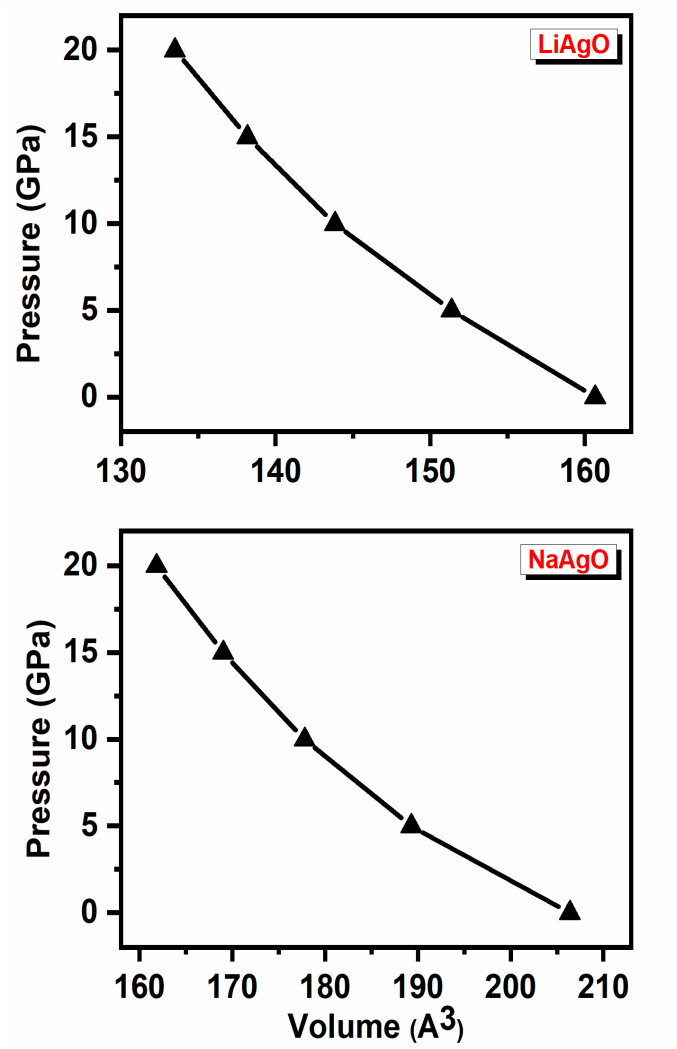

Fig. 2. Computed pressure versus primitive-cell volume data for the LiAgO and NaAgO materials. The symbols are the calculated results and the continuous lines are Birch EOS fits.

III.2.2 Electronic properties

For better understanding of the electronic and optical properties of these compounds, the investigation of the electronic eigen energies E as a function of the wave vector k (E(k)), in the first Brillouin zone (BZ), would be useful. We have calculated the energy band structure E(k) on a discrete k-mesh following high-symmetry directions in the k-space at the equilibrium lattice parameters within the GGA-PBE for the LiAgO and NaAgO compounds. The obtained results are depicted in Fig. 3. The energy values were gauged to ensure that the highest energy for a valence electron is exactly equal to 0 eV. The obtained fundamental energy band gaps for the BAgO (B = Li, Na) compounds are summarized in Table 2, along with the available theoretical results [7] for the sake of comparison. We are not aware of any optical spectroscopic measurements of the gaps for the studied materials. It is a well-known problem that both LDA and GGA approximations usually underestimate the band gap when using self-consistent band structure calculations within DFT [9, 10].Typically, in the DFT calculation the underestimation of the band gap when compared with experimental data is about 30–100% [11]. This is mainly due to the fact that they have simple forms that are not sufficiently flexible for accurately reproducing both exchange–correlation energy and its charge derivative. So, the herein studied materials would have gap higher values than those obtained using DFT within GGA and LDA approximations. As seen from Fig. 3, the two considered materials have an indirect band gap (Z–Γ) and the value of the fundamental band gap decreases when the atomic number Z of the B atom increases. Our calculated energy band gap values are somewhat larger than those reported in Ref. [7]. This is probably due to the use of a different ab initio method (TB-LMTO within the LDA) by Umamaheswari and co-workers [7]; their method is known to underestimate the energy band gap value compared to the GGA used in the present work. Our predicted indirect band gap character (Z–Γ) for LiAgO and NaAgO is in agreement with the prediction of Ref. [7]. Our calculations have predicted an indirect band gap (Z–Γ) for the two studied compounds; however, there are some differences on how this ‘‘indirect character’’ of the band gap is formed in these two materials. The enlarged view of the band gaps of these materials (Fig. 4) clearly illustrates these differences. For example, the top of the valence band of NaAgO is very flat near the Z point and this flatness decreases going from NaAgO to LiAgO. The energy of the direct transition (Γ–Γ) decreases in the following sequence: LiAgO → NaAgO. Since the value of the fundamental indirect band gap (Z–Γ) also decreases, so the difference between these two bands gaps decreases; this is clearly shown in Fig. 4. It can be seen that the energy of the BZX

point in the valence bands becomes progressively closer to the Fermi level in the following sequence: LiAgO → NaAgO.

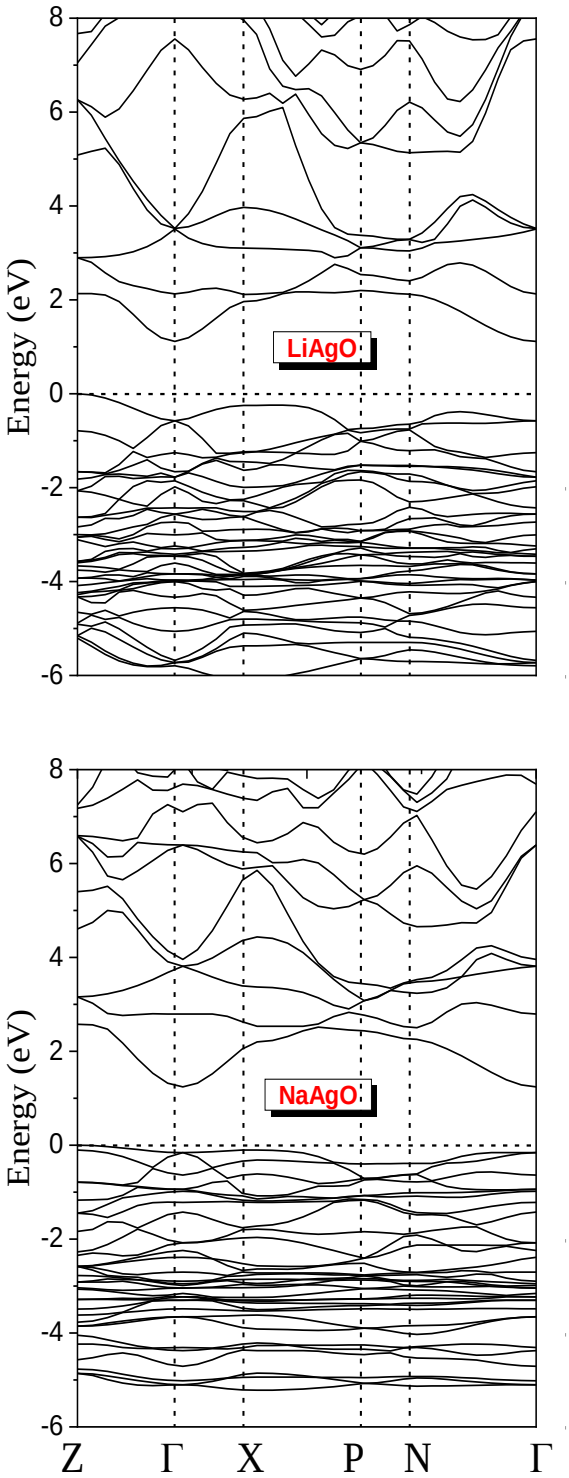

Fig. 3. Calculated band structure dispersion curves for the LiAgO and NaAgO materials along high symmetry directions in the Brillouin zone.

Table 2: Calculated direct and indirect band gap values and the *UVBW* for the LiAgO and NaAgO compounds, using the GGA-PBE methods.

	Z - Z	Γ - Γ	X - X	P - P	N - N	Γ- Z	Γ- X	Γ- P	Γ- N
LiAgO									
GGA-WC	2.17857	1.305	2.2558	2.94781	2.7604	1.125	1.202	2.72084	2.65168
NaAgO									
GGA-WC	2.63572	1.39	2.36966	2.79643	2.61014	1.240	1.32	2.54518	2.36387

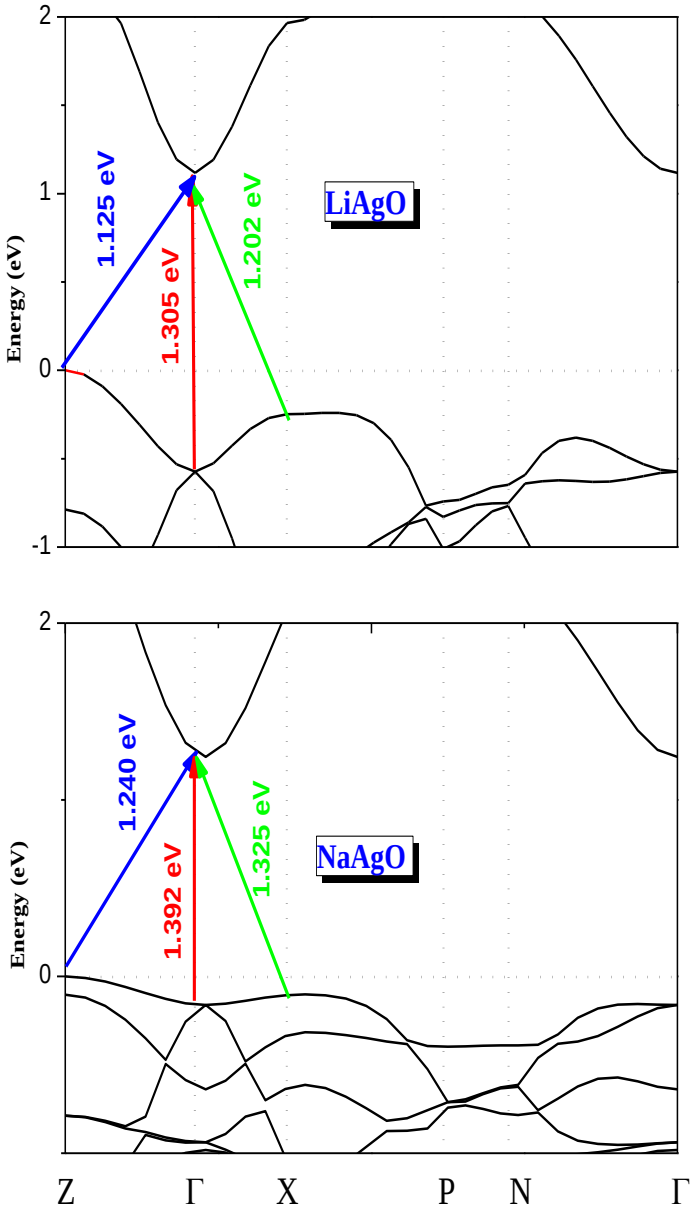

Fig. 4. Enlarged view of the band structure around the fundamental band gap with indication of the values of the fundamental energy band Z– Γ, energy of the direct transition Γ – Γ and energy of the indirect transition X – Γ for the LiAgO and NaAgO materials. gap.

In order to understand the origin of the important band structure features of the herein studied materials, we must consider the relative contributions of each atom species to the density of electronic states. Partial density of states (PDOS) and total density of states (TDOS) diagrams for the BAgO compounds are depicted in Fig. 5. These diagrams allow us to conclude that the lowest conduction band is formed by the hybridization of the O-2p states and the Ag-P band and Na-P appear inside the lowest conduction band of LiAgO and NaAgO, respectively. The upper valence bands consist of one manifold in the LiAgO, while they split into two sub-bands in NaAgO. This can be clearly seen in the band structures shown in Fig. 3. The upper one arises from the hybridization of Ag-3d states and O-2p states, suggesting the presence of a covalent bonding character between O and Ag atoms

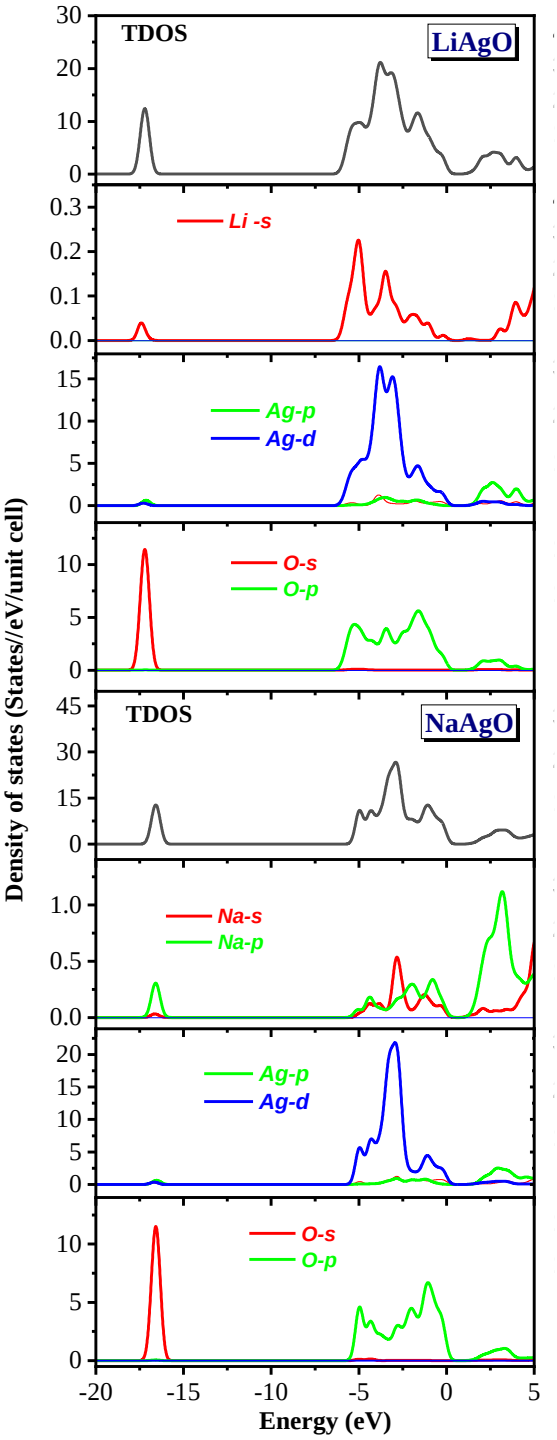

Fig. 5. Total and site projected densities of states (TDOS and PDOS, respectively) for the LiAgO and NaAgO materials.

III.2.3 Optical properties

One of the main optical parameter of a material is its dielectric function, $\varepsilon(\omega) = \varepsilon_1(\omega) + i\varepsilon_2(\omega)$, because it is the fundamental feature of the linear response to an electromagnetic wave. The imaginary part $\varepsilon_2(\omega)$ of the dielectric function

can be computed from the electronic band structure by calculating the momentum matrix elements between the occupied and unoccupied wave functions respecting the selection rules [12]:

$$\varepsilon_2(\omega) = \frac{Ve^2}{2\pi\hbar m^2\omega^2}\int d^3k \sum_{nn'} \left|\langle kn|\, p\,|kn'\rangle\right|^2 f(kn)\times[1-f(kn')]\,\delta(E_{kn}-E_{kn'}-\hbar\omega) \qquad \text{(III.1)}$$

In this expression, $<f\ |p_\alpha\ |i>$ and $<f|p_\beta|i>$ are the dipole matrix elements corresponding to the α and β directions of the crystal (*x*, *y* or *z*), and *f*, *i* are the final and initial states, respectively. W_n is the Fermi distribution function for the *n* th state and E_n is the electron energy in the *n* th state. The real part of the frequency-dependent dielectric function expression $\varepsilon_{\alpha\beta}(\omega)$ can be numerically calculated from $\varepsilon_2^{\alpha\beta}(\omega)$ using the Kramers–Kronig transform:

$$\varepsilon_1(\omega) = 1 + \frac{2}{\pi}\mathrm{P}\int_0^\infty \frac{\omega'\varepsilon_2(\omega')}{\omega'^2-\omega^2}\mathrm{d}\omega' \qquad \text{(III.2)}$$

, Where *P* is the Cauchy principal value of the integral. The other optical constants, such as the refractive index $n(\omega)$, the extinction coefficient $k(\omega)$, the reflectivity $R(\omega)$ and the loss function $L(\omega)$, can be calculated from the dielectric function $\varepsilon(\omega)=\varepsilon_1(\omega)+i\varepsilon_2(\omega)$ using the following relations:

$$n(\omega) = \left[\frac{\varepsilon_1(\omega)}{2} + \frac{\sqrt{\varepsilon_1^{\,2}(\omega)\ +\varepsilon_2^{\,2}(\omega)}}{2}\right]^{1/2} \qquad \text{(III.3)}$$

$$k(\omega) = \left[-\frac{\varepsilon_1(\omega)}{2} + \frac{\sqrt{\varepsilon_1^{\,2}(\omega)\ +\varepsilon_2^{\,2}(\omega)}}{2}\right]^{1/2} \qquad \text{(III.4)}$$

$$R(\omega) = \left|\frac{\varepsilon(\omega)^{0.5}-1}{\varepsilon(\omega)^{0.5}+1}\right|^2 \qquad \text{(III.5)}$$

$$L(\omega) = \left|\frac{\varepsilon_2(\omega)}{\varepsilon_1^2(\omega)+\varepsilon_2^2(\omega)}\right| \qquad \text{(III.6)}$$

It is worth to note here that the approach implemented in CASTEP code to calculate $\varepsilon_2(\omega)$ has some limitations. First of all, the local field effects (related to the fact that the electric field experienced at a particular site of a crystal is screened by the polarizability of the atom at this site) are neglected. Second, phonon contributions to the optical spectra, which are

especially important for the crystals with indirect gap, are not taken into account. However, even with these limitations, it has been reported in the literature [13–16] that the calculated spectra for different materials are generally in a reasonable agreement with the experimental ones.

The computed absorptive ($\varepsilon_2(\omega)$) and dispersive parts ($\varepsilon_1(\omega)$) of the complex dielectric functions ($\varepsilon(\omega)$) are displayed in Fig. 6, as a function of the photon energy for the two studied compounds. Due to the tetragonal structure of the studied materials, optical spectra were calculated for incident light polarized along the [100] and [001] crystalline directions. The instrumental smearing of 0.1 eV was used to model the broadening effects. In spite of the anisotropy in the structural properties, we find that both the real $\varepsilon_1$and the imaginary ε_2 parts of the dielectric function do not demonstrate any optical anisotropy. The behavior of $\varepsilon_2(\omega)$ is rather similar for all the studied compounds with some small differences. This is attributed to the fact that the band structures of these materials are similar with minor differences causing insignificant changes in the structures of $\varepsilon_2(\omega)$. The prominent structures in $\varepsilon_2(\omega)$ spectrum are mainly ascribed to the transitions from O-2p and Ag-2d states in the valence bands to A-p and Ag-3p states in the conduction bands.

The real parts $\varepsilon_1(\omega)$, in the limit of zero energy values (the infinite wavelengths) i.e. the so-called static dielectric constant $\varepsilon_1(0)$, are 6.50, 5.50 for the LiAgO and NaAgO, materials respectively.

The refractive index *n(ω)* and extinction coefficient *k(ω)* of the BAgO (B = Li, Na) compounds are displayed in Fig. 7. The calculated zero energy ($\lambda=\infty$) *n(0)* values for the LiAgO and NaAgO, compounds are equal to 2.50 and 2.33 respectively. The energies for which the dispersion is null, E(n = 1), are equal to 7.79 and 6.82 eV for LiAgO and NaAgO respectively.

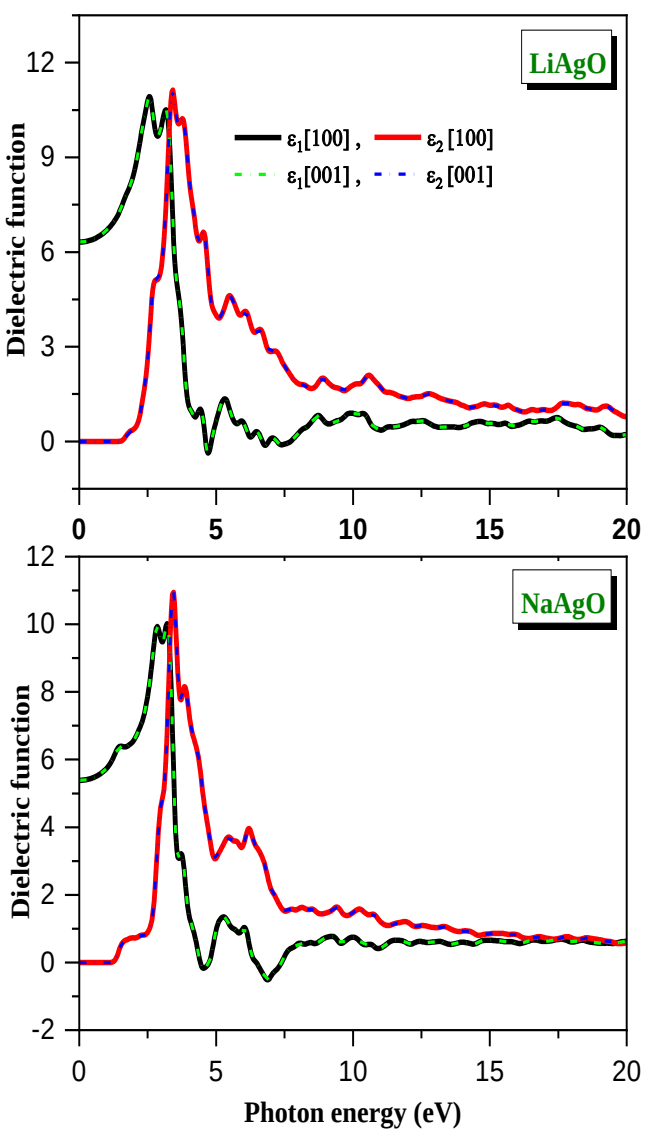

Fig. 6. calculated imaginary part $\varepsilon_2(\omega)$ and real part $\varepsilon_1(\omega)$ of the dielectric function $\varepsilon(\omega)$for two different directions of the incident light polarization for the LiAgO and NaAgO compounds.

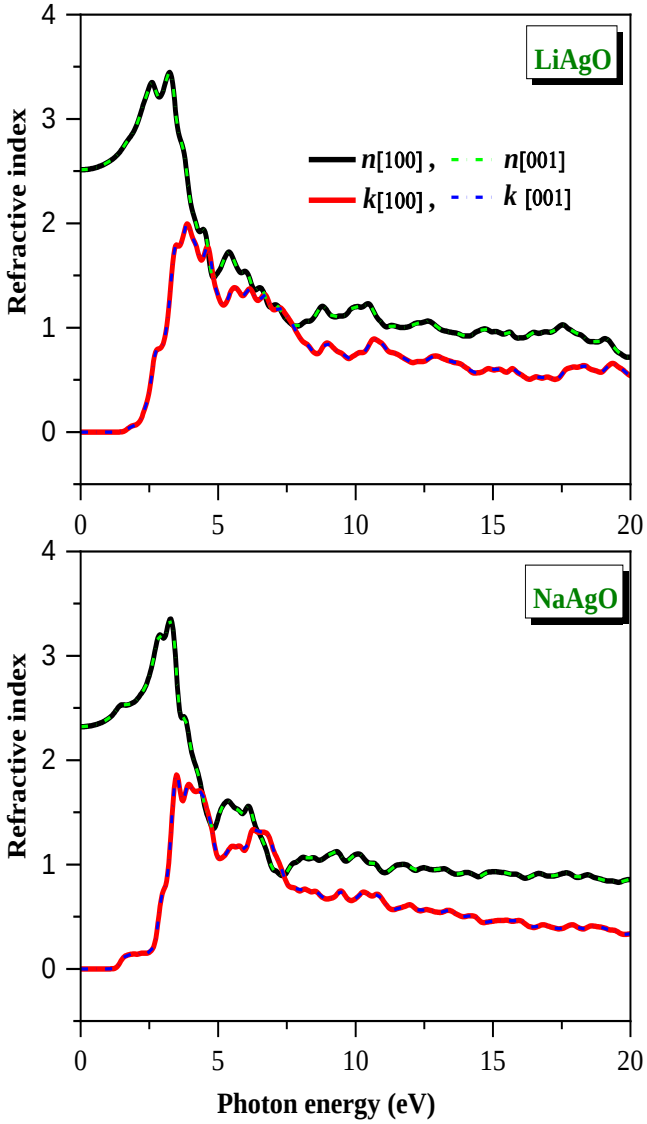

Fig. 7. Calculated refractive index n(x) and extinction coefficient k(x) spectra for the LiAgO, NaAgO materials.

In Fig. 8, we show the reflectivity spectra *R(ω)* for the herein studied materials. The *R(ω)* values of these compounds do not approach the unity when the light frequency ω tends to zero, which means that these compounds behave like semiconductors. In Fig. 8, we present the electron energy loss functions *L(ω)*. The *L(ω)* function is an important factor describing the energy loss of a fast electron traversing a material. The peaks in *L(ω)* spectra is associated with the plasma resonance and the corresponding frequency is the so-called plasma frequency ω_p. The peaks of *L(ω)* correspond to the trailing edges in the reflection spectra. We do not find optical data in the literature for the BAgO (B = Li and Na) compounds, and we hope that our calculations will lead to further experimental efforts on these materials. By combining the

measured data with the calculation results, a near total understanding of the electronic and optical properties of the herein studied materials is possible.

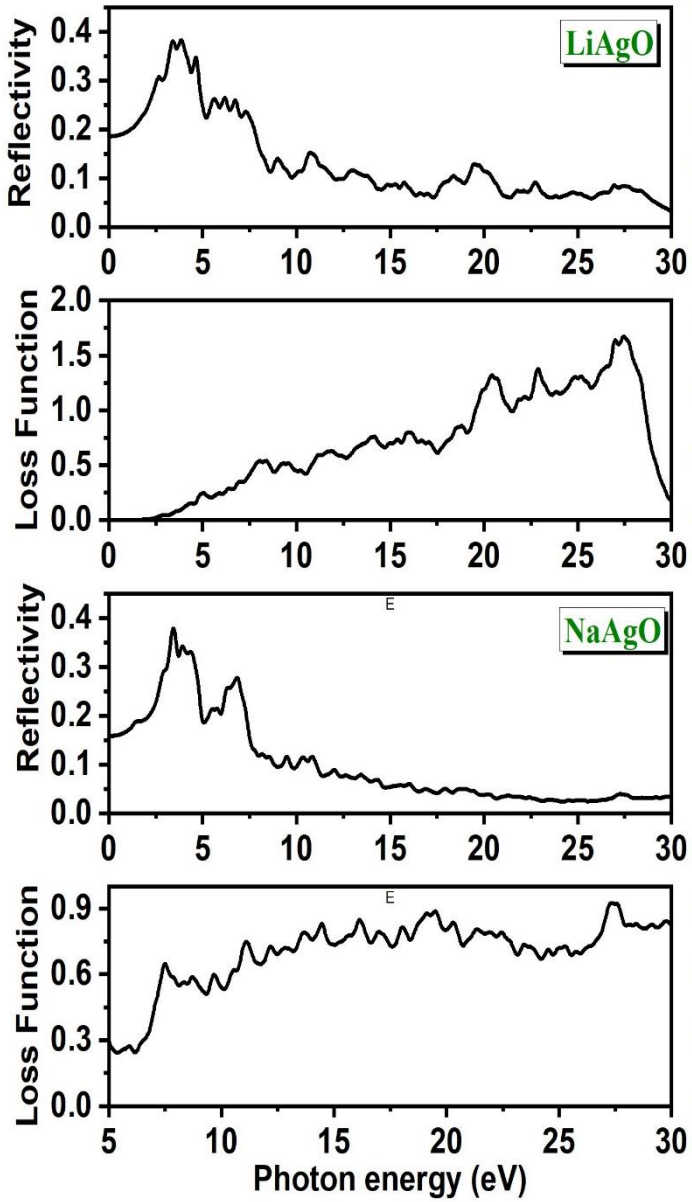

Fig. 8. Calculated reflectivity coefficient R(ω) and loss function L(ω) spectra for the LiAgO and NaAgO materials.

Reference:

[1] S.J. Clark, M.D. Segall, C.J. Pickard, P.J. Hasnip, M.J. Probert, K. Refson, M.C. Payne, Zeitschrift fuer Kristallographie 220 (2005) 567.

[2] J.P. Perdew, S. Burke, M. Ernzerhof, Phys. Rev. Lett. 77 (1996) 3865.

[3] D. Vanderbilt, Phys. Rev. B 41 (1990) 7892.

[4] H.J. Monkhorst, J.D. Pack, Phys. Rev. B 13 (1976) 5188.

[5] T.H. Fischer, J. Almlof, J. Phys. Chem. 96 (1992) 9768

[6] D. Fischer, W. Carl, H. Glaum, R. Hoppe, Z. Anorg, Allg. Chem. 585 (1990) 75.

[7] R. Umamaheswari, M. Yogeswari, G. Kalpana, Solid State Commun. 155 (2013)62.

[8] F. Birch, J. Geophys. Res. 83 (1978) 1257.

[9] A. Ghafari, A. Boochani, C. Janowitz, R. Manzke, Phys. Rev. B 84 (2011) 125205.

[10] P. Dufek, P. Blaha, K. Schwarz, Phys. Rev. 50 (1994) 7279.

[11] C.S. Wang, W.E. Pickett, Phys. Rev. Lett. 51 (1983) 597.

[12] X. Guo, J. He, Y. Tian, Phys. Rev. B 73 (2006) 045108.

[13] R.S. Mulliken, J. Chem. Phys. 23 (1955) 1833.

[14] F.L. Hirshfeld, Theor. Chim. Acta 44 (1977) 129.

[15] A.M. Silva, B.P. Silva, F.A.M. Sales, V.N. Freire, E. Moreira, U.L. Fulco, E.L.Albuquerque, Phys. Rev. B 86 (2012) 195201.

[16] R.K. Roy, K. Hirao, S. Krishnamurty, S. Pal, J. Chem. Phys. 115 (2001) 2901.

[17] R.K. Roy, S. Pal, K. Hirao, J. Chem. Phys. 110 (1999) 8236.

[18] R.G. Parr, W.T. Yang, J. Am. Chem. Soc. 106 (1984) 4049.

[19] L. Makinistian, E.A. Albanesi, Phys. Rev. B 74 (2006) 045206.

[20] M.G. Brik, J. Phys. Chem. Solids 71 (2010) 1435.

[21] R. Shirley, M. Kraft, O.R. Inderwildi, Phys. Rev. B 81 (2010) 075111.

[22] L. Tingyu, S. Jianqi, Z. Qiren, Solid State Commun. 135 (2005) 382.

[23] L. Tingyu, S. Jianqi, Z. Qiren, Z. Songlin, J. Lumin. 126 (2007) 239.

General Conclusions

In this work, we have performed ab initio calculations of the structural, electronic and optical properties for the tetragonal BAgO (B = Li and Na) compounds. Our optimized lattice parameters are in good agreement with the existing experimental data. We have found an anisotropic behavior of the pressure dependence of the lattice constants. We have found that these materials are indirect band gap semiconductors. The fundamental band gap value decreases with the increase of the atomic number Z of the alkaline metal B. The BAgO compounds are found to be optically isotropic though they are structurally and elastically anisotropic. Some macroscopic optical constants have been predicted in the 0–20 eV energy range. As far as the BAgO (A = Li and Na) compounds are concerned, our results for the optical properties are predictions, and we welcome experiments to prove them.

ملخص

لقد قمنا في هذه المذكرة بدراسة الخواص البنيوية، الالكترونية، الضوئية، للمركبات LiAgO و NaAgO باستعمال طريقة الأمواج المستوية مع الكمون الزائف في إطار نظرية دالية الكثافة الالكترونية (DFT)،المدمجة في برنامج CASTEP. لقد استعملنا تقريب التدرج المعمم (GGA-PBE) لمعالجة كمون تبادل-ارتباط (XC)من أجل حساب الخواص البنيوية و الالكترونية و الضوئية.

يمكن تلخيص النتائج المتحصل عليها فيمايلي:

- هناك توافق جيد بين نتائج حسابات المعاملات البنيوية (ثوابت الشبكة البلورية، احداثيات الذرات و معامل الانضغاط B ومشتق معامل الانضغاط B') للحالة الأساسية مع النتائج التجريبية و النظرية المتوفرة في المنشورات العلمية.
- بينت نتائج الحسابات أن المواد المدروسة تنتمي لعائلة أنصاف النواقل بموانع طاقة أساسية غير مباشرة Z–Γ .
- تم حساب الجزء التخيلي $\varepsilon_2(\omega)$ و الجزء الحقيقي $\varepsilon_1(\omega)$ لدالة السماحية $\varepsilon(\omega)$،الانعكاسية $R(\omega)$ ،قرينة الانكسار $n(\omega)$ ، معامل الخمود $K(\omega)$ ، دالة ضياعالطاقة الالكترونية $L(\omega)$ و معامل الامتصاص $\alpha(\omega)$ في مجال طاقوي من 0 إلى 20eV.

a b s t r a c t

Ab initio total energy calculations were performed to study in details the structural, electronic and optical properties of Ag-based ternary oxides BAgO (A B= Li and Na). Optimized atomic coordinates and lattice constants agree well with the existing experimental and theoretical data. Band structure, total and site-projected l-decomposed densities of states, charge transfers and charge density distribution maps were obtained; analyzed and compared with the available theoretical data. Complex dielectric function, refractive index, extinction coefficient, reflectivity and loss function spectra were calculated with an incident radiation polarized parallel to both [100] and [001] crystalline directions.